

# Spatial Scattering Modulation with Multipath Component Aggregation

Jiliang Zhang, *Senior Member IEEE*, Wei Liu, *Senior Member IEEE*, Alan Tennant, *Senior Member IEEE*,  
Weijie Qi, Jiming Chen, and Jie Zhang, *Senior Member IEEE*

**Abstract**—In this paper, a multipath component aggregation (MCA) mechanism is introduced for spatial scattering modulation (SSM) to overcome the limitation in conventional SSM that the transmit antenna array steers the beam to a single multipath (MP) component at each instance. In the proposed MCA-SSM system, information bits are divided into two streams. One is mapped to an amplitude-phase-modulation (APM) constellation symbol, and the other is mapped to a beam vector symbol which steers multiple beams to selected strongest MP components via an MCA matrix. In comparison with the conventional SSM system, the proposed MCA-SSM enhances the bit error performance by avoiding both low receiving power due to steering the beam to a single weak MP component and inter-MP interference due to MP components with close values of angle of arrival (AoA) or angle of departure (AoD). For the proposed MCA-SSM, a union upper bound (UUB) on the average bit error probability (ABEP) with any MCA matrix is analytically derived and validated via Monte Carlo simulations. Based on the UUB, the MCA matrix is analytically optimized to minimize the ABEP of the MCA-SSM. Finally, numerical experiments are carried out, which show that the proposed MCA-SSM system remarkably outperforms the state-of-the-art SSM system in terms of ABEP under a typical indoor environment.

**Index Terms**—Spatial scattering modulation, analogue beam-forming, MIMO, intelligent ray launching, indoor radio wave propagation, bit error probability.

## I. INTRODUCTION

Index modulation (IM) with sparse symbol mapping has been considered as a promising candidate to facilitate 5G/B5G point-to-point connections [1]–[8]. Recently, spatial scattering modulation (SSM) has been proposed as an attractive solution for IM with millimeter wave (mmWave) multiple-input-multiple-output (MIMO) antenna arrays at both the transmitter (Tx) and the receiver (Rx) [9]–[11]. The SSM system requires fewer radio frequency (RF) chains at the Tx to reduce power

consumption by steering the beam to one selected multipath (MP) components.

In a conventional SSM system, the information bits are separated into two streams. The first stream is mapped to an amplitude-phase-modulation (APM) constellation symbol, while the second one is mapped to one of the MP components with the largest gains in the wireless channel according to the input bits.

Recently, SSM has drawn much attention as a strong candidate for 5G/B5G modulation systems with various extensions. S. Ruan et al. analytically derived the diversity order of the conventional SSM system [12]. Q. Li et al. explored how to effectively exploit the polarization domain resource to design a polarized SSM [13]. J. Zhang et al. developed an adaptive SSM scheme to maximize the data rate constrained by a maximal tolerable bit error probability [14]. Y. Ding et al. extended the SSM to the generalized SSM (GSSM) by configuring multiple RF chains by allowing acceptable hardware overhead [15]. S. Guo further analyzed the spectral efficiency of GSSM and emphasized it as a breakthrough in mmWave MIMO [16]. J. Yan et al. applied the GSSM system in a 3-D MIMO scheme, and validated the performance of 3-D GSSM [17].

However, the above SSM systems suffer from two problems. One is the risk of low receiving power as the transmitter may steer the beam to an MP component with a low cluster gain with a large path loss; the other is the inter-MP interference because the values of angle of arrival (AoA)/angle of departure (AoD) for different MP components could be too close for the receiver/transmitter to resolve. In [19], [20], signal shaping mechanisms are introduced to address the above problems via a recursive optimization approach at the cost of a heavy computational burden.

Therefore, the main objective of this paper is to propose an analytic MP component aggregation (MCA) mechanism in the design of SSM to overcome both above problems. On the one hand, the proposed MCA-SSM increases the possible minimal received power by aggregating multiple MP components for an overall large gain. On the other hand, MP components are aggregated in an orthogonal manner to avoid selecting two MP components with close AoAs or AoDs. Moreover, an analytic MCA matrix derivation approach is presented instead of through recursive optimization, which leads to reduced computational complexity for its implementation. Therefore, the proposed MCA-SSM is expected to outperform the conventional SSM system in terms of average bit error probability (ABEP).

The main contributions of this paper are summarized as

Corresponding Author: Wei Liu (w.liu@qmul.ac.uk).

Jiliang Zhang is with College of Information Science and Engineering, Northeastern University, Shenyang, China. Wei Liu is with the School of Electronic Engineering and Computer Science, Queen Mary University of London, UK. Jie Zhang is with the Department of Electronic and Electrical Engineering, The University of Sheffield, Sheffield, UK, and also with Ranplan Wireless Network Design Ltd., Cambridge, UK. Alan Tennant is with the Department of Electronic and Electrical Engineering, The University of Sheffield, Sheffield, UK. Weijie Qi and Jiming Chen are with Ranplan Wireless Network Design Ltd., Cambridge, UK.

This research was a part of KTP project - “Massive MIMO Beamforming for 5G”, which is funded by UKRI through Innovate UK. Jiliang Zhang would also like to acknowledge the support from the National Key R&D Program of China (Grant No. 2021YFB3300900). Wei Liu would also like to acknowledge the support from the UK Engineering and Physical Sciences Research Council (Grant No. EP/V009419/1)

TABLE I  
NOTATIONS IN THIS PAPER.

Notations	Definitions	Notations	Definitions
$N_t$	Number of Tx antenna elements	$N_r$	Number of Rx antenna elements
$n_t$	Index of transmit antenna elements	$n_r$	Index of receive antenna elements
$\mathbf{W}$	The MCA matrix	$\mathbf{H}$	The MIMO channel matrix
$N_{ts}$	Total number of multipath components	$\tilde{\mathbf{H}}_{n_s}$	Channel matrix of the $n_s$ -th MP component
$\mathbf{a}_t$	Array steering vector at the transmitter	$\mathbf{a}_r$	Array steering vector at the receiver
$\boldsymbol{\theta}_t$	The AoD of multipath components	$\boldsymbol{\theta}_r$	The AoA of multipath components
$\boldsymbol{\beta}$	The channel gain of multipath components	$\mathbf{G}$	Effective channel matrix
$N_s$	Total number of applied multipath components	$N_{s,a}$	Total number of applied orthogonal subchannels
$M$	Modulation order of APM symbols	$L$	Total number of beam vector symbols
$m$	Index of APM symbols	$l$	Index of beam vector symbols
$\mathbf{x}$	The transmitted signal vector	$\mathbf{y}$	The received signal vector
$(\cdot)^H$	Complex conjugate transpose operator	$\odot$	Hadamard product
$\boldsymbol{\lambda}$	Eigenvalues of $\mathbf{G}^H \mathbf{G}$	$\mathbf{U}$	Eigenvectors of $\mathbf{G}^H \mathbf{G}$
$\kappa$	Index of subchannels	$\boldsymbol{\xi}$	Weighting factors of subchannels
$\text{chol}(\cdot)$	Cholesky factorization of a matrix	$\text{Tr}(\cdot)$	Trace of a matrix
$R \nmid I$	$R$ is indivisible by $I$	$ \cdot $	Magnitude of each complex element in the array
$E[\cdot]$	Expectation operator	$Q(\cdot)$	The $Q$ -function

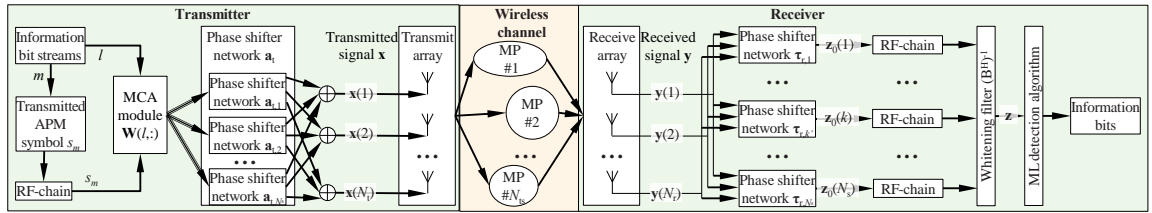


Fig. 1. System model of the proposed MCA-SSM.

follows:

- An MCA mechanism is introduced in the state-of-the-art SSM system, as shown in Fig. 1. Therein, MP components in the wireless channel can be aggregated via the MCA matrix  $\mathbf{W}$  into several beam patterns. At each instance, one of the beam patterns, associated with one row of the MCA matrix, is selected according to the input bits.
- To facilitate optimization of the bit error performance for the MCA-SSM system, a quick evaluation approach for the MCA-SSM system is designed. More specifically, a tight union upper bound (UUB) on the ABEP for an MCA-SSM system with an arbitrary MCA matrix is derived and validated via Monte-Carlo simulations.
- The optimization problem for the MCA matrix is formulated to minimize the ABEP of the proposed MCA-SSM based on the UUB. Therein, the MCA matrix is constructed pursuing orthogonality to circumvent analytical intractability. The sub-optimal MCA matrix is analytically derived as a solution to a set of linear equations. The simple expression of the MCA matrix facilitates easy implementation of MCA-SSM.
- A systematic evaluation of the proposed MCA-SSM system is demonstrated in a typical indoor environment based on an intelligent ray launching algorithm (IRLA). Numerical results show that the proposed MCA-SSM system significantly outperforms the conventional SSM system.

The rest of this paper is structured as follows. The system model of the proposed MCA-SSM is described in Section II,

where the MCA matrix is defined. With an arbitrary MCA matrix, the UUB on the ABEP of the MCA-SSM system is derived in Section III. In Section IV, an analytical MCA mechanism is proposed to solve the optimization problem. Section V provides a case study on how to apply results in Section IV with given channel parameters. Then, the performance is further validated in a stochastic channel model with randomly distributed channel parameters. A systematic evaluation of the proposed MCA-SSM system in a typical indoor environment is presented in Section VI. Finally, conclusions are drawn in Section VII.

Notations of this paper are summarized in TABLE I.

## II. SYSTEM MODEL

This section introduces the system model of the proposed MCA-SSM as shown in Fig. 1.

### A. Model assumptions

**Assumption 1:** We consider a point-to-point connection with MIMO antenna arrays at both the Tx and the Rx. The Tx array and the Rx array have  $N_t$  and  $N_r$  elements, respectively. The transmission from the Tx array to the Rx array can be expressed as

$$\mathbf{y} = \sqrt{\frac{\rho}{N_t}} \mathbf{H} \mathbf{x} + \mathbf{n}_a, \quad (1)$$

where  $\rho$  is the SNR at the receiver,  $\mathbf{H}$  is the  $N_r \times N_t$  channel matrix,  $\mathbf{x}$  is the  $N_t \times 1$  transmitted signal vector,  $\mathbf{y}$  is the  $N_r \times 1$  received signal vector, and  $\mathbf{n}_a \sim \mathcal{CN}(\mathbf{0}, \mathbf{I})$  is the  $N_r \times 1$  noise vector.  $\mathbf{H}$  is normalized to  $E[\text{Tr}(\mathbf{H}^H \mathbf{H})] = N_t N_r$ .

**Assumption 2:** Perfect channel state information (CSI) is assumed to be known at both the Tx and the Rx following the setup of typical SSM systems [9]–[15], [17], [19], [20].

**Assumption 3:** The narrowband sparse physical channel is adopted in this paper [9]. A link-level indoor channel is composed by  $N_{ts}$  MP components with different channel gains, AoDs, and AoAs. The channel matrix is given by [25]

$$\mathbf{H} = \sum_{n_s=1}^{N_{ts}} \beta(n_s) \tilde{\mathbf{H}}_{n_s}, \quad (2)$$

where  $\beta$  is the  $N_{ts} \times 1$  descending sorted channel gain vector. Its  $n_s$ -th element, denoted by  $\beta(n_s)$ , is the channel gain from the Tx array to the Rx array via the  $n_s$ -th MP component.  $\tilde{\mathbf{H}}_{n_s}$  is the normalized channel matrix from the Tx array to the Rx array via the  $n_s$ -th MP component.

$$\tilde{\mathbf{H}}_{n_s} = \mathbf{a}_{r,n_s} \mathbf{a}_{t,n_s}^H, \quad (3)$$

$\mathbf{a}_{t,n_s}$  and  $\mathbf{a}_{r,n_s}$  are Tx and Rx array steering vectors, respectively, which are both column vectors [9].

**Assumption 4:** For simplicity, assume that both the Tx and the Rx are equipped with uniform linear antenna arrays (ULAs) and all elements are omnidirectional and unpolarized. The  $n_t$ -th element of  $\mathbf{a}_{t,n_s}$  and the  $n_r$ -th element of  $\mathbf{a}_{r,n_s}$  are, respectively, given by

$$\mathbf{a}_{t,n_s}(n_t) = e^{j \frac{2\pi}{\eta} (n_t - \frac{1+N_t}{2}) d_t \cos \theta_t(n_s)}, \quad (4)$$

and

$$\mathbf{a}_{r,n_s}(n_r) = e^{j \frac{2\pi}{\eta} (n_r - \frac{1+N_r}{2}) d_r \cos \theta_r(n_s)}, \quad (5)$$

where  $\eta$  denotes wavelength of the radio wave.  $\theta_t$  is the  $N_{ts} \times 1$  AoD vector. Its  $n_s$ -th element, denoted by  $\theta_t(n_s)$ , is the AoD of the  $n_s$ -th MP component. Similarly,  $\theta_r$  is the AoA vector.  $d_t$  and  $d_r$  denote adjacent spacing of Tx and Rx antenna elements, respectively.

## B. Transmitter

In the proposed MCA-SSM system, information bits are divided into two streams to be transmitted at each instance. The total data rate is  $R = R_{mp} + R_{sy} = \log_2(ML)$  bits/symbol, where  $M$  is the modulation order of the APM and  $L$  is the number of candidate beam vector symbols.

To transmit the first stream,  $s_m$  is selected from an APM constellation with  $M$  candidate symbols, such as  $M$ -phase shift keying ( $M$ -PSK) and quadrature amplitude modulation ( $M$ -QAM). As such, the data rate of the first stream is  $R_{sy} = \log_2 M$ .

To transmit the second stream, a beam vector symbol out of  $L$  MCA candidate beam vector symbols is selected to generate a beam pattern steering to  $N_s$  strongest MP components. As such, the data rate of the second stream is  $R_{mp} = \log_2 L$ .

The MCA mechanism for the second stream is illustrated in Fig. 1, and further elaborated as follows. When  $N_{ts}$  MP components are available in the wireless channel, Tx generates a beam pattern steering to  $N_s$  candidate MP components out of  $N_{ts}$  MP components at any instance. We choose MP components with  $N_s$  greatest channel gain to maximize the

received power. For each selected MP component out of the  $N_s$  strongest ones, a transmit phase shifter network is applied to steer a pencil beam to it based on the analog beamforming approach. With **Assumption 2**, the Tx knows the number of MP components  $N_{ts}$ , the gain of all selected MP components  $\beta(1 : N_s)$ , as well as their AoAs  $\theta_t(1 : N_s)$  and AoDs  $\theta_r(1 : N_s)$ . Then, the response of the  $k$ -th phase shifter network is given by  $\mathbf{a}_{t,k}^H$ , where  $k \in 1, 2, \dots, N_s$ . To aggregate the  $N_s$  strongest MP components, we use an MCA matrix  $\mathbf{W}$  to weight and divide the power of the APM signal into  $N_s$  signals, and feed them into the  $N_s$  phase shifter networks. If  $R_{mp}$  bits are transmitted in the second bit stream,  $L = 2^{R_{mp}}$  rows of the MCA matrix  $\mathbf{W}$  are candidates to be selected from. As such,  $\mathbf{W}$  is an  $L \times N_s$  matrix. With the energy conservation law,  $\mathbf{W}$  is normalized to  $\|\mathbf{W}(l, :)\|^2 = 1$  throughout this paper. The design of  $\mathbf{W}$  will be elaborated in Section IV.

Based on the above MCA mechanism, the overall response of the MCA matrix and all phase shifter networks at Tx is calculated by

$$\boldsymbol{\tau}_{t,l} = \sum_{k=1}^{N_s} \mathbf{W}^*(l, k) \mathbf{a}_{t,k} = [\mathbf{W}(l, :)] \mathbf{A}_t(1 : N_s, :)]^H, \quad (6)$$

where

$$\mathbf{A}_t = \begin{bmatrix} \mathbf{a}_{t,1}^H \\ \mathbf{a}_{t,2}^H \\ \vdots \\ \mathbf{a}_{t,N_{ts}}^H \end{bmatrix}. \quad (7)$$

Therefore, the transmitted signal at all Tx antenna elements, i.e.,  $\mathbf{x}$  in (1), is

$$\begin{aligned} \mathbf{x} &= \boldsymbol{\tau}_{t,l} s_m = \sum_{k=1}^{N_s} \mathbf{W}^*(l, k) \mathbf{a}_{t,k} s_m \\ &= [\mathbf{W}(l, :)] \mathbf{A}_t(1 : N_s, :)]^H s_m. \end{aligned} \quad (8)$$

## C. Receiver

At the Rx, the received signal is computed by substituting (8) into (1).

$$\mathbf{y} = \sqrt{\frac{\rho}{N_t}} \mathbf{H} [\mathbf{W}(l, :)] \mathbf{A}_t(1 : N_s, :)]^H s_m + \mathbf{n}_a. \quad (9)$$

With **Assumption 3**, we have

$$\begin{aligned} \mathbf{y} &= \sqrt{\frac{\rho}{N_t}} \sum_{n_s=1}^{N_{ts}} \beta(n_s) \mathbf{a}_{r,n_s} \mathbf{a}_{t,n_s}^H [\mathbf{W}(l, :)] \mathbf{A}_t(1 : N_s, :)]^H s_m \\ &\quad + \mathbf{n}_a. \end{aligned} \quad (10)$$

The received signal  $\mathbf{y}$  is filtered by  $N_s$  Rx phase shifter networks and fed into  $N_s$  Rx RF chains. By assuming that Rx knows perfect CSI via channel estimation, each pair of Rx phase shifter network and Rx RF-chain is associated with one candidate MP component. To maximize the SNR at the RF chain, each Rx phase shifter network steers a pencil beam to its associated candidate MP component. That is, for the  $k'$ -th candidate MP component, the Rx phase shifter network is set as  $\mathbf{a}_{r,k'}$ .

Denote the output signal of RF chains as  $\mathbf{z}_0$ . Then, the output signal of the  $k'$ -th RF chain,  $\mathbf{z}_0(k')$ , is computed by multiplying both sides of (10) by  $\mathbf{a}_{r,k'}$ , as in (11), and then,

$$\mathbf{z}_0 = \sqrt{\rho} \bar{\mathbf{H}}_0(:, l) s_m + \mathbf{n}_{\text{RF}}. \quad (12)$$

To simplify the derivation of the optimal detection algorithm, an  $N_s \times L$  effective channel matrix  $\bar{\mathbf{H}}_0$  is defined in (11). Following some algebraic manipulations,  $\bar{\mathbf{H}}_0$  is given by

$$\begin{aligned} \bar{\mathbf{H}}_0 &= \sqrt{\frac{1}{N_t}} \mathbf{A}_r(1 : N_s, :) \\ &\times \sum_{n_s=1}^{N_{ts}} \beta(n_s) \mathbf{a}_{r,n_s} \mathbf{a}_{t,n_s}^H \mathbf{A}_t^H(1 : N_s, :), \end{aligned} \quad (13)$$

where

$$\mathbf{A}_r = \begin{bmatrix} \mathbf{a}_{r,1}^H \\ \mathbf{a}_{r,2}^H \\ \vdots \\ \mathbf{a}_{r,N_{ts}}^H \end{bmatrix}. \quad (14)$$

Moreover, since  $\mathbf{n}_{\text{RF}}$  is not white when  $\mathbf{n}_a$  is white, the covariance matrix of  $\mathbf{n}_{\text{RF}}$ , denoted by  $\mathbf{C}_{\text{noise}} \triangleq \mathbb{E}[\mathbf{n}_{\text{RF}} \mathbf{n}_{\text{RF}}^H]$  can be computed by

$$\mathbf{C}_{\text{noise}}(k, k') = \mathbb{E}[\mathbf{n}_{\text{RF}}(k) \mathbf{n}_{\text{RF}}^H(k')] = \mathbb{E}[\mathbf{n}_a^H \mathbf{a}_{r,k} \mathbf{a}_{r,k'}^H \mathbf{n}_a], \quad (15)$$

and thus

$$\mathbf{C}_{\text{noise}} = \mathbf{A}_r(1 : N_s, :)\mathbf{A}_r^H(1 : N_s, :), \quad (16)$$

which is not an identity matrix.

To whiten the noise, we multiply both sides of (12) by  $(\mathbf{B}^H)^{-1}$ , where matrix  $\mathbf{B}$  is obtained by Cholesky factorization of  $\mathbf{C}_{\text{noise}}$ , i.e.,  $\mathbf{B} = \text{chol}(\mathbf{C}_{\text{noise}})$  [17]. Then, we have

$$\mathbf{z} = (\mathbf{B}^H)^{-1} \mathbf{z}_0 = \sqrt{\rho} \mathbf{G} \mathbf{W}^H(l, :) s_m + \underbrace{(\mathbf{B}^H)^{-1} \mathbf{n}_{\text{RF}}}_{\mathcal{CN}(\mathbf{0}, \mathbf{I})}, \quad (17)$$

where  $\mathbf{G}$  is an  $N_s \times N_s$  matrix and computed by

$$\begin{aligned} \mathbf{G} &= \sqrt{\frac{1}{N_t}} (\mathbf{B}^H)^{-1} \mathbf{A}_r(1 : N_s, :) \\ &\times \sum_{n_s=1}^{N_{ts}} \beta(n_s) \mathbf{a}_{r,n_s} \mathbf{a}_{t,n_s}^H \mathbf{A}_t^H(1 : N_s, :). \end{aligned} \quad (18)$$

Equation (17) is the same as the system model for conventional spatial modulation (SM) with equivalent channel matrix  $\mathbf{G} \mathbf{W}^H$  and additive white Gaussian noise  $(\mathbf{B}^H)^{-1} \mathbf{n}_{\text{RF}}$  [18, Eq. (1)]. Then, applying a whitening filter and with the maximal likelihood (ML) detection, the optimal MCA-SSM detector is given by [23, Eq. (4)]

$$[\hat{l}, \hat{m}] = \arg \min_{l, m} \{ \|\mathbf{z} - \sqrt{\rho} \mathbf{G} \mathbf{W}^H(l, :) s_m\| \}. \quad (19)$$

**Remark 1.** It is worth noting that the proposed MCA-SSM system is a generalization of state-of-the-art SSM [9]–[11]. For  $N_s = L$ , the proposed system is reduced to the SSM system [9]–[11] if  $\mathbf{W} = \mathbf{I}$ . The MCA mechanism is applicable in the GSSM system [15], [17] as well. The approach is to combine this work and the GSM proposed in [38], [39].

### III. BIT ERROR PROBABILITY ANALYSIS AND PROBLEM FORMULATION

It is well known that analytical derivation of the exact ABEP with fading channels for complex modulation systems is challenging. Therefore, a tight UUB on the ABEP for a given channel matrix  $\mathbf{H}$  is derived as [24]

$$\begin{aligned} \text{ABEP}_{\mathbf{H}} &\leq \sum_{l_1=1}^L \sum_{l_2=1}^L \sum_{m_1=1}^M \sum_{m_2=1}^M \\ &\times \frac{N(l_1, m_1, l_2, m_2) P_{\text{EP}, \mathbf{H}}(l_1, m_1, l_2, m_2)}{LM \log_2(LM)}, \end{aligned} \quad (20)$$

where  $N(l_1, m_1, l_2, m_2)$  denotes the number of bits in error when  $l_1$  and  $m_1$  are transmitted at Tx but  $l_2$  and  $m_2$  are detected at Rx.  $P_{\text{EP}, \mathbf{H}}(l_1, m_1, l_2, m_2)$  is the pairwise error probability, defined as the probability that, when  $l_1$  and  $m_1$  are transmitted but  $l_2$  and  $m_2$  are detected assuming only candidates  $(l_1, m_1)$  and  $(l_2, m_2)$  can be selected at Tx. A closed-form expression of  $P_{\text{EP}, \mathbf{H}}(l_1, m_1, l_2, m_2)$  can be computed by

$$P_{\text{EP}, \mathbf{H}}(l_1, m_1, l_2, m_2) = Q \left( \sqrt{\frac{\rho J_{l_1, m_1, l_2, m_2}}{2}} \right), \quad (21)$$

where  $J_{l_1, m_1, l_2, m_2}$  is the Euclidean distance (ED) between  $\mathbf{G} \mathbf{W}^H(l_1, :) s_{m_1}$  and  $\mathbf{G} \mathbf{W}^H(l_2, :) s_{m_2}$ , given by

$$\begin{aligned} J_{l_1, m_1, l_2, m_2} &\triangleq \|\mathbf{G} \mathbf{W}^H(l_1, :) s_{m_1} - \mathbf{G} \mathbf{W}^H(l_2, :) s_{m_2}\|^2 \\ &= (\mathbf{W}^H(l_1, :) s_{m_1} - \mathbf{W}^H(l_2, :) s_{m_2})^H \mathbf{G}^H \\ &\quad \times \mathbf{G} (\mathbf{W}^H(l_1, :) s_{m_1} - \mathbf{W}^H(l_2, :) s_{m_2}). \end{aligned} \quad (22)$$

In this paper, we design the MCA mechanism by maximizing the minimum ED [19], [20], which determines the ABEP in the high-SNR regime [12], [21]. Therefore, the optimization problem is formulated as

$$\begin{aligned} &\text{maximize} \quad \min_{\substack{(l_1, m_1) \neq (l_2, m_2) \\ 1 \leq l_1 \leq L, l_1 \in \mathbb{N}^+ \\ 1 \leq m_1 \leq M, m_1 \in \mathbb{N}^+ \\ 1 \leq l_2 \leq L, l_2 \in \mathbb{N}^+ \\ 1 \leq m_2 \leq M, m_2 \in \mathbb{N}^+}} J_{l_1, m_1, l_2, m_2}, \\ &\text{s.t.} \quad \|\mathbf{W}(l, :)\| = 1, \forall l. \end{aligned} \quad (23)$$

$$\begin{aligned} \mathbf{z}_0(k') &= \mathbf{a}_{r, k'}^H \mathbf{y} \\ &= \underbrace{\sqrt{\rho} \mathbf{a}_{r, k'}^H \sqrt{\frac{1}{N_t}} \sum_{n_s=1}^{N_{ts}} \beta(n_s) \mathbf{a}_{r, n_s} \mathbf{a}_{t, n_s}^H \sum_{k=1}^{N_s} \mathbf{W}^*(l, k) \mathbf{a}_{t, k} s_m}_{\bar{\mathbf{H}}_0(k', l)} + \underbrace{\mathbf{a}_{r, k'}^H \mathbf{n}_a}_{\mathbf{n}_{\text{RF}}(k')} \\ &= \sqrt{\rho} \bar{\mathbf{H}}_0(k', l) s_m + \mathbf{n}_{\text{RF}}(k'). \end{aligned} \quad (11)$$

Apply eigendecomposition to  $\mathbf{G}^H\mathbf{G}$ , and we have

$$\mathbf{G}^H\mathbf{G} = \mathbf{U}\mathbf{\Lambda}\mathbf{U}^H, \quad (24)$$

where  $\mathbf{U}$  is a uniform matrix, and  $\mathbf{U}^H\mathbf{U} = \mathbf{I}$ .  $\mathbf{\Lambda}$  is a real diagonal matrix with descending-sorted eigenvalues  $\lambda_1, \lambda_2, \dots, \lambda_{N_s}$ .

By substituting (24) into (22) and defining  $\mathbf{V} \triangleq (\mathbf{U}\mathbf{W})^H$  we have

$$\begin{aligned} J_{l_1, m_1, l_2, m_2} &= (\mathbf{V}(:, l_1)_{s_{m_1}} - \mathbf{V}(:, l_2)_{s_{m_2}})^H \\ &\quad \times \mathbf{\Lambda}(\mathbf{V}(l_1, :)_{s_{m_1}} - \mathbf{V}(l_2, :)_{s_{m_2}}) \\ &= \sum_{\kappa=1}^{N_s} \lambda_{\kappa} |\mathbf{V}(\kappa, l_1)_{s_{m_1}} - \mathbf{V}(\kappa, l_2)_{s_{m_2}}|^2 \\ &= \lambda |\mathbf{V}(l_1, :)_{s_{m_1}} - \mathbf{V}(l_2, :)_{s_{m_2}}|^2, \end{aligned} \quad (25)$$

where  $\lambda \triangleq [\lambda_1, \lambda_2, \dots, \lambda_{N_s}]$ . Under a given channel matrix, i.e., given  $\lambda_{\kappa}$  and  $\mathbf{U}$ , we need to design the MCA matrix  $\mathbf{W}$  to achieve a low ABEP calculated by (20).

Noting that we can design  $\mathbf{V}$  instead of  $\mathbf{W}$ , and obtain  $\mathbf{W}$  by  $\mathbf{W} = (\mathbf{V}\mathbf{U})^H$ , the optimization problem in (23) is reformulated as (26).

Therein, the constraint  $\|\mathbf{V}(l, :)\| = 1, \forall l$  is applied to guarantee that  $\|\mathbf{W}(l, :)\| = 1, \forall l$ , as  $\mathbf{U}$  is a uniform matrix, and  $\mathbf{W} = \mathbf{V}^H\mathbf{U}$ .

#### IV. PROPOSED MULTIPATH COMPONENT AGGREGATION MECHANISM

In this section, we propose an approach to solve (26). It is worth noting that obtaining optimal solution of (26) is still challenging. Numerous techniques may be invoked for constructing the sub-optimal matrix  $\mathbf{V}$  for the classic SM systems [19], [20], [36], [37]. Different from the SM system, the channel in (2) is sparse and the eigenvalues  $\lambda$  differ from each other a lot. Therefore, we apply  $N_{s,a}$  subchannels with

the greatest eigenvalues to compose  $\mathbf{V}$  as follows<sup>1</sup>.

$$\mathbf{V}(l, :) = (\mathbf{v}_l \odot \boldsymbol{\xi})^H, \quad (27)$$

where  $\odot$  denotes the Hadamard product,  $\mathbf{v}_l$  is a vector that is associated with the  $l$ -th beam vector symbol,  $\|\mathbf{v}_l\| = 1, \forall l$ ,  $\boldsymbol{\xi}$  is a real weighting factor that allocates power to subchannels with various eigenvalues,  $\|\boldsymbol{\xi}\| = 1$ , and

$$\begin{aligned} \mathbf{V}(l, (N_{s,a} + 1) : N_s) &= \mathbf{v}_l((N_{s,a} + 1) : N_s) \\ &= \boldsymbol{\xi}((N_{s,a} + 1) : N_s) = 0, \forall l. \end{aligned} \quad (28)$$

**Example 1.** Learning from PSK, design of  $\mathbf{v}_l$  can be achieved as follows with  $N_{s,a} = 2$ .

$$\mathbf{v}_l = \left[ \cos\left(\frac{\pi}{4} + \frac{(l-1)\pi}{L}\right), \sin\left(\frac{\pi}{4} + \frac{(l-1)\pi}{L}\right), 0, \dots, 0 \right]. \quad (29)$$

For example, if  $L = 2$ , we have

$$\begin{cases} \mathbf{v}_1 = \left[ \frac{1}{\sqrt{2}}, \frac{1}{\sqrt{2}}, 0, 0 \right], \\ \mathbf{v}_2 = \left[ -\frac{1}{\sqrt{2}}, \frac{1}{\sqrt{2}}, 0, 0 \right]. \end{cases} \quad (30)$$

If  $L = 4$ , we have

$$\begin{cases} \mathbf{v}_1 = \left[ \frac{1}{\sqrt{2}}, \frac{1}{\sqrt{2}}, 0, 0 \right], \\ \mathbf{v}_2 = [0, 1, 0, 0], \\ \mathbf{v}_3 = \left[ -\frac{1}{\sqrt{2}}, \frac{1}{\sqrt{2}}, 0, 0 \right], \\ \mathbf{v}_4 = [1, 0, 0, 0]. \end{cases} \quad (31)$$

By substituting (27) into (26) and following some straightforward algebraic manipulations, the optimization problem can be rewritten as (32). The reformulated optimization problem in (32) facilitates an analytic solution for the matrix  $\mathbf{V}$ , which is given by Theorems 1 and 2 for PSK and QAM signal constellations, respectively.

<sup>1</sup>Besides tractability, another benefit is the simplification of the detection algorithm given by (19), which can be reformulated as  $[\hat{l}, \hat{m}] = \arg \min_{l, m} \left\{ \sum_{\kappa=1}^{N_{s,a}} |\mathbf{z}(\kappa) - \sqrt{\rho\lambda_{\kappa}}\boldsymbol{\xi}(\kappa)\mathbf{v}_l(\kappa)s_m|^2 \right\}$ , as  $\|\mathbf{z} - \sqrt{\rho}\mathbf{G}\mathbf{W}^H(l, :)_s\|^2 = \sum_{\kappa=1}^{N_{s,a}} |\mathbf{z}(\kappa) - \sqrt{\rho\lambda_{\kappa}}\boldsymbol{\xi}(\kappa)\mathbf{v}_l(\kappa)s_m|^2$ . As such, i) the detector does not need to compute  $\mathbf{z}((N_{s,a} + 1) : N_s)$  and ii) the number of items in the summation is reduced from  $N_s$  to  $N_{s,a}$ . Thus, the computational burden of the detection algorithm can be further reduced.

$$\begin{aligned} &\text{maximize} \quad \min_{\substack{(l_1, m_1) \neq (l_2, m_2) \\ 1 \leq l_1 \leq L, l_2 \in \mathbb{N}^+ \\ 1 \leq m_1 \leq M, m_2 \in \mathbb{N}^+ \\ 1 \leq l_2 \leq L, l_2 \in \mathbb{N}^+ \\ 1 \leq m_2 \leq M, m_2 \in \mathbb{N}^+}} \{ \lambda |\mathbf{V}(l_1, :)_{s_{m_1}} - \mathbf{V}(l_2, :)_{s_{m_2}}|^2 \}, \\ &\text{s.t.} \quad \|\mathbf{V}(l, :)\| = 1, \forall l. \end{aligned} \quad (26)$$

$$\begin{aligned} &\text{maximize} \quad \min_{\substack{(l, m) \neq (\hat{l}, \hat{m}) \\ 1 \leq l_1 \leq L, l_2 \in \mathbb{N}^+ \\ 1 \leq m_1 \leq M, m_2 \in \mathbb{N}^+ \\ 1 \leq l_2 \leq L, l_2 \in \mathbb{N}^+ \\ 1 \leq m_2 \leq M, m_2 \in \mathbb{N}^+}} \left\{ \sum_{\kappa=1}^{N_{s,a}} \boldsymbol{\xi}^2(\kappa) \lambda_{\kappa} |\mathbf{v}_{l_1}(\kappa)s_{m_1} - \mathbf{v}_{l_2}(\kappa)s_{m_2}|^2 \right\}, \\ &\text{s.t.} \quad \|\boldsymbol{\xi}\| = 1. \end{aligned} \quad (32)$$

**Theorem 1. Analytic solution of the optimization problem (32) for PSK signal constellation.** The solution of (32) is computed by

$$\xi = \sqrt{\frac{[1, \iota_{\text{opt},2}, \dots, \iota_{\text{opt},N_{s,a}}, 0, \dots, 0]}{1 + \sum_{\kappa=2}^{N_{s,a}} \iota_{\text{opt},\kappa}}}, \quad (33)$$

where  $\iota_{\text{opt}} = [1, \iota_{\text{opt},2}, \dots, \iota_{\text{opt},N_{s,a}}]$  is one of  $\iota_{[n_{e,1}, n_{e,2}, \dots, n_{e,N_{s,a}-1}]}$  that maximizes the minimal  $J_{l_1, m_1, l_2, m_2}$  via traversing all possible  $[n_{e,1}, n_{e,2}, \dots, n_{e,N_{s,a}-1}]$  satisfying  $n_{e,1} < n_{e,2} < \dots < n_{e,N_{s,a}-1}$ .  $\iota_{[n_{e,1}, n_{e,2}, \dots, n_{e,N_{s,a}-1}]}$  is the solution to the equation

$$\epsilon_{n_{e,1}} \iota^T = \epsilon_{n_{e,2}} \iota^T = \dots = \epsilon_{n_{e,n_{s,a}}} \iota^T = \dots = \epsilon_{n_{e,N_{s,a}-1}} \iota^T, \quad (34)$$

$\epsilon_{n_{e,n_{s,a}}}$  is an array with  $N_{s,a}$  elements, chosen from the set  $\mathcal{D}$  without replacement.  $\mathcal{D}$  is given by

$$\mathcal{D} = \mathcal{D}_0 - \{\epsilon \in \mathcal{D}_0, \epsilon(\kappa) \geq \epsilon'(\kappa), \forall \kappa, \exists \epsilon' \in \mathcal{D}_0, \epsilon' \neq \epsilon\}. \quad (35)$$

For PSK signal constellation,  $\mathcal{D}_0$  is defined by (36).

*Proof:* See Appendix A. ■

**Theorem 2. Analytic solution of the optimization problem (32) for QAM signal constellation.**

For QAM signal constellation, the solution of (32) is computed by (32)-(35) as well but  $\mathcal{D}_0$  in (35) is computed as follows.

For square QAM signal constellation,  $\mathcal{D}_0$  is defined by (37), where  $\mathcal{S}_m$  is given by (38). For rectangular QAM signal constellation,  $\mathcal{D}_0$  is defined by (39), where  $\mathcal{S}_m$  is given by (40).

Noting that  $\mathcal{S}_m$  needs to be deduced for MCA-SSM with QAM constellation diagrams. Specifically,  $\mathcal{S}_m$  for  $M = 8, 16, 32, 64$  are summarized in TABLE 2.

*Proof:* See Appendix A. ■

## V. CASE STUDY

### A. Cases under consideration

To clearly explain how to apply Theorem 1 and Theorem 2 in the proposed MCA-SSM system, we consider Example 2 and Example 3 for 16-PSK and 16-QAM, respectively, with  $N_{s,a} = 2$ ,  $L = 4$ , and  $M = 16$ . Then,  $\mathbf{v}_l$  is given by (31). For other values of  $N_s$ ,  $N_{s,a}$ ,  $L = 4$ , and  $M$ , Theorem 1 and Theorem 2 can be applied using a similar approach.

$$\begin{aligned} \mathcal{D}_0 = & \underbrace{\left\{ 4 \sin^2 \left( \frac{\pi}{M} \right) \lambda(1 : N_{s,a}) \odot |\mathbf{v}_{l_1}(1 : N_{s,a})|^2 \mid 1 \leq l_1 \leq L, l_1 \in \mathbb{N}^+ \right\}}_{\mathcal{D}_1} \\ & \cup \underbrace{\left\{ \lambda(1 : N_{s,a}) \odot (\mathbf{v}_{l_1}(1 : N_{s,a}) \pm \mathbf{v}_{l_2}(1 : N_{s,a}))^2 \mid \substack{1 \leq l_1 \leq L, l_1 \in \mathbb{N}^+ \\ l_1 < l_2 \leq L, l_2 \in \mathbb{N}^+} \right\}}_{\mathcal{D}_2}. \end{aligned} \quad (36)$$

$$\begin{aligned} \mathcal{D}_0 = & \underbrace{\left\{ \frac{6\lambda(1 : N_{s,a}) \odot |\mathbf{v}_{l_1}(1 : N_{s,a})|^2}{M-1} \mid 1 \leq l_1 \leq L, l_1 \in \mathbb{N}^+ \right\}}_{\mathcal{D}_1} \\ & \cup \underbrace{\left\{ \lambda(1 : N_{s,a}) \odot |\mathbf{v}_{l_1}(1 : N_{s,a})s_{m_1} \pm \mathbf{v}_{l_2}(1 : N_{s,a})s_{m_2}|^2 \mid \substack{1 \leq l_1 \leq L, l_1 \in \mathbb{N}^+ \\ l_1 < l_2 \leq L, l_2 \in \mathbb{N}^+ \\ (s_{m_1}, s_{m_2}) \in \mathcal{S}_m} \right\}}_{\mathcal{D}_2}. \end{aligned} \quad (37)$$

$$\mathcal{S}_m = \left\{ (s_1, s_2) \mid \begin{array}{l} s_1 = \sqrt{\frac{3}{2(M-1)}}(R_1 + I_1), s_2 = \sqrt{\frac{3}{2(M-1)}}(R_2 + I_2) \\ R_1 \in \{1, 3, 5, \dots, \sqrt{M}-1\}, I_1 \in \{1, 3, 5, \dots, R_1\}, \\ R_2 \in \{1, 3, 5, \dots, R_1\}, I_2 \in \{1, 3, 5, \dots, I_1\}, \\ R_1 \nmid I_1, \forall (R_1 \neq 1), R_2 \nmid I_2, \forall (R_2 \neq 1), \\ s_1 \neq s_2, \forall (R_1, I_1) \neq (1, 1) \end{array} \right\}. \quad (38)$$

$$\begin{aligned} \mathcal{D}_0 = & \underbrace{\left\{ \frac{24\lambda(1 : N_{s,a}) \odot |\mathbf{v}_{l_1}(1 : N_{s,a})|^2}{5M-4} \mid 1 \leq l_1 \leq L, l_1 \in \mathbb{N}^+ \right\}}_{\mathcal{D}_1} \\ & \cup \underbrace{\left\{ \lambda(1 : N_{s,a}) \odot |\mathbf{v}_{l_1}(1 : N_{s,a})s_{m_1} \pm \mathbf{v}_{l_2}(1 : N_{s,a})s_{m_2}|^2 \mid \substack{1 \leq l_1 \leq L, l_1 \in \mathbb{N}^+ \\ l_1 < l_2 \leq L, l_2 \in \mathbb{N}^+ \\ (s_{m_1}, s_{m_2}) \in \mathcal{S}_m} \right\}}_{\mathcal{D}_2}. \end{aligned} \quad (39)$$

$$\mathcal{S}_m = \left\{ (s_1, s_2) \mid \begin{array}{l} s_1 = \sqrt{\frac{6}{5M-4}}(R_1 + I_1), s_2 = \sqrt{\frac{6}{5M-4}}(R_2 + I_2) \\ R_1 \in \{1, 3, 5, \dots, \sqrt{2M}-1\}, I_1 \in \{1, 3, 5, \dots, \min\{R_1, \sqrt{M/2}-1\}\}, \\ R_2 \in \{1, 3, 5, \dots, R_1\}, I_2 \in \{1, 3, 5, \dots, I_1\}, \\ R_1 \nmid I_1, \forall R_1 \neq 1, R_2 \nmid I_2, \forall R_2 \neq 1, \\ s_1 \neq s_2, \forall (R_1, I_1) \neq (1, 1) \end{array} \right\}. \quad (40)$$

Channel parameters for both examples are listed in TABLE III. We further assign  $N_s = 4$ . With these channel parameters, we can obtain that  $\boldsymbol{\lambda} = [410.05, 9.84, 1.41, 0.05]$  and

$$\mathbf{U} = \begin{bmatrix} 0.0697 & -0.6370 & 0.0568 & 0.7656 \\ 0.0275 & 0.7688 & -0.0187 & 0.6386 \\ -0.3857 & -0.0558 & -0.9192 & 0.0569 \\ -0.9196 & -0.0019 & 0.3892 & 0.0533 \end{bmatrix} = \begin{bmatrix} \mathbf{u}_1 \\ \mathbf{u}_2 \\ \mathbf{u}_3 \\ \mathbf{u}_4 \end{bmatrix}. \quad (41)$$

**Example 2. 16-PSK signal constellation.**

Firstly, as  $|\mathbf{v}_1(1)|^2 = |\mathbf{v}_1(2)|^2 = |\mathbf{v}_3(1)|^2 = |\mathbf{v}_3(2)|^2 = 1/2$ ,  $|\mathbf{v}_2(1)|^2 = |\mathbf{v}_4(2)|^2 = 1$ ,  $|\mathbf{v}_2(2)|^2 = |\mathbf{v}_4(1)|^2 = 0$ , and  $\sin^2(\frac{\pi}{16}) = \frac{1}{4}(2 - \sqrt{2 + \sqrt{2}})$  we obtain  $\mathcal{D}_1$  as (42).

Secondly, we obtain  $\mathcal{D}_2$  as (43) based on (44) and (45).

Then, combining (42) and (43), and with  $(2 - \sqrt{2 + \sqrt{2}}) < 4$ ,  $(2 - \sqrt{2 + \sqrt{2}}) < (1 - \frac{1}{\sqrt{2}})^2$ ,  $(2 - \sqrt{2 + \sqrt{2}}) < \frac{1}{2}$ , we have

$$\mathcal{D} = \left\{ \begin{array}{l} \left(1 - \sqrt{\frac{2+\sqrt{2}}{4}}\right) [\lambda_1, \lambda_2], \\ \left(2 - \sqrt{2 + \sqrt{2}}\right) [\lambda_1, 0], \\ \left(2 - \sqrt{2 + \sqrt{2}}\right) [0, \lambda_2], \end{array} \right\} \quad (46)$$

According to Theorem 1, the solution of (32) is one of the following equations.

$$\begin{cases} \left(1 - \sqrt{\frac{2+\sqrt{2}}{4}}\right) (\lambda_2 \lambda_2 + \lambda_1) = \left(2 - \sqrt{2 + \sqrt{2}}\right) \lambda_1, \\ \left(2 - \sqrt{2 + \sqrt{2}}\right) \lambda_2 \lambda_2 = \left(2 - \sqrt{2 + \sqrt{2}}\right) \lambda_1. \end{cases} \quad (47)$$

Therefore, the only possible solution is

$$l_{\text{opt},2} = \frac{\lambda_1}{\lambda_2} \quad (48)$$

By substituting (48) into (32) and with some straightforward derivations, we obtain

$$\boldsymbol{\xi}^2 = \left[ \frac{\lambda_2}{\lambda_1 + \lambda_2}, \frac{\lambda_1}{\lambda_1 + \lambda_2} \right], \quad (49)$$

$$\mathbf{V} = \begin{bmatrix} \frac{1}{\sqrt{2}} \sqrt{\frac{\lambda_2}{\lambda_1 + \lambda_2}} & \frac{1}{\sqrt{2}} \sqrt{\frac{\lambda_1}{\lambda_1 + \lambda_2}} & 0 & 0 \\ 0 & \sqrt{\frac{\lambda_1}{\lambda_1 + \lambda_2}} & 0 & 0 \\ -\frac{1}{\sqrt{2}} \sqrt{\frac{\lambda_2}{\lambda_1 + \lambda_2}} & \frac{1}{\sqrt{2}} \sqrt{\frac{\lambda_1}{\lambda_1 + \lambda_2}} & 0 & 0 \\ \sqrt{\frac{\lambda_2}{\lambda_1 + \lambda_2}} & 0 & 0 & 0 \end{bmatrix}, \quad (50)$$

and thus

$$\mathbf{W} = \begin{bmatrix} \frac{1}{\sqrt{2}} \sqrt{\frac{\lambda_2}{\lambda_1 + \lambda_2}} \mathbf{u}_1 + \frac{1}{\sqrt{2}} \sqrt{\frac{\lambda_1}{\lambda_1 + \lambda_2}} \mathbf{u}_2 \\ \sqrt{\frac{\lambda_1}{\lambda_1 + \lambda_2}} \mathbf{u}_2 \\ -\frac{1}{\sqrt{2}} \sqrt{\frac{\lambda_2}{\lambda_1 + \lambda_2}} \mathbf{u}_1 + \frac{1}{\sqrt{2}} \sqrt{\frac{\lambda_1}{\lambda_1 + \lambda_2}} \mathbf{u}_2 \\ \sqrt{\frac{\lambda_2}{\lambda_1 + \lambda_2}} \mathbf{u}_1 \end{bmatrix}. \quad (51)$$

**Example 3.  $N_{s,a} = 2$ ,  $L = 4$ , 16-QAM signal constellation.**

For the 16-QAM signal constellation,

$$\mathcal{D}_1 = \left\{ \frac{1}{5} [\lambda_1, \lambda_2], \frac{2}{5} [\lambda_1, 0], \frac{2}{5} [0, \lambda_2] \right\}. \quad (52)$$

Then,

$$\mathcal{S}_m = \left\{ \sqrt{\frac{1}{10}} (1 + j, 1 + j), \sqrt{\frac{1}{10}} (1 + j, 3 + j) \right\}, \quad (53)$$

and we have  $\mathcal{D}_2$  in (54).

$$\mathcal{D}_1 = \left\{ \left(1 - \sqrt{\frac{2+\sqrt{2}}{4}}\right) [\lambda_2, \lambda_1], \left(2 - \sqrt{2 + \sqrt{2}}\right) [\lambda_1, 0], \left(2 - \sqrt{2 + \sqrt{2}}\right) [0, \lambda_2] \right\}. \quad (42)$$

$$\mathcal{D}_2 = \left\{ [4\lambda_1, 0], [0, 4\lambda_2], \left[\left(1 - \frac{1}{\sqrt{2}}\right)^2 \lambda_1, \frac{1}{2} \lambda_2\right], \left[\frac{1}{2} \lambda_1, \left(1 - \frac{1}{\sqrt{2}}\right)^2 \lambda_2\right] \right\}. \quad (43)$$

$$\begin{aligned} & \left\{ \boldsymbol{\lambda}(1 : N_{s,a}) \odot (\mathbf{v}_{l_1}(1 : N_{s,a}) - \mathbf{v}_{l_2}(1 : N_{s,a}))^2 \Big|_{\substack{1 \leq l_1 \leq L, l_1 \in \mathbb{N}^+ \\ l_1 < l_2 \leq L, l_2 \in \mathbb{N}^+}} \right\} \\ & = \left\{ [4\lambda_1, 0], \left[\left(1 - \frac{1}{\sqrt{2}}\right)^2 \lambda_1, \frac{1}{2} \lambda_2\right], \left[\frac{1}{2} \lambda_1, \left(1 - \frac{1}{\sqrt{2}}\right)^2 \lambda_2\right] \right\}. \end{aligned} \quad (44)$$

$$\begin{aligned} & \left\{ \boldsymbol{\lambda}(1 : N_{s,a}) \odot (\mathbf{v}_{l_1}(1 : N_{s,a}) + \mathbf{v}_{l_2}(1 : N_{s,a}))^2 \Big|_{\substack{1 \leq l_1 \leq L, l_1 \in \mathbb{N}^+ \\ l_1 < l_2 \leq L, l_2 \in \mathbb{N}^+}} \right\} \\ & = \left\{ [0, 4\lambda_2], \left[\left(1 - \frac{1}{\sqrt{2}}\right)^2 \lambda_1, \frac{1}{2} \lambda_2\right], \left[\frac{1}{2} \lambda_1, \left(1 - \frac{1}{\sqrt{2}}\right)^2 \lambda_2\right] \right\}. \end{aligned} \quad (45)$$

$$\mathcal{D}_2 = \left\{ \begin{array}{l} \frac{2}{5} [\lambda_1, 0], \frac{2}{5} [0, \lambda_2], \frac{1}{5} \left[\left(1 - \frac{1}{\sqrt{2}}\right)^2 \lambda_1, \frac{1}{2} \lambda_2\right], \frac{1}{5} \left[\frac{1}{2} \lambda_1, \left(1 - \frac{1}{\sqrt{2}}\right)^2 \lambda_2\right], \\ \frac{1}{10} \left[\frac{|1+3j|^2}{2} \lambda_1, \left|(1+j) - \frac{1+3j}{\sqrt{2}}\right|^2 \lambda_2\right], \frac{1}{10} \left[\left|(1+j) - \frac{1+3j}{\sqrt{2}}\right|^2 \lambda_1, \frac{|1+3j|^2}{2} \lambda_2\right], \\ \frac{1}{10} \left[\frac{|1+j|^2}{2} \lambda_1, \left|(1+3j) - \frac{1+j}{\sqrt{2}}\right|^2 \lambda_2\right], \frac{1}{10} \left[\left|(1+3j) - \frac{1+j}{\sqrt{2}}\right|^2 \lambda_1, \frac{|1+j|^2}{2} \lambda_2\right] \end{array} \right\}. \quad (54)$$

TABLE II  
 $\mathcal{S}_m$  FOR TYPICAL QAM CONSTELLATIONS.

Signal constellation	$\mathcal{S}_m$
8-QAM	$\left\{ \sqrt{\frac{1}{6}}(1+j, 1+j), \sqrt{\frac{1}{6}}(1+j, 3+j) \right\}$
16-QAM	$\left\{ \sqrt{\frac{1}{10}}(1+j, 1+j), \sqrt{\frac{1}{10}}(1+j, 3+j) \right\}$
32-QAM	$\left\{ \begin{array}{l} \sqrt{\frac{1}{26}}(1+j, 1+j), \sqrt{\frac{1}{26}}(1+j, 3+j), \sqrt{\frac{1}{26}}(1+j, 5+j), \sqrt{\frac{1}{26}}(1+j, 5+3j), \\ \sqrt{\frac{1}{26}}(1+j, 7+j), \sqrt{\frac{1}{26}}(1+j, 7+3j), \sqrt{\frac{1}{26}}(3+j, 5+j), \sqrt{\frac{1}{26}}(3+j, 5+3j), \\ \sqrt{\frac{1}{26}}(3+j, 7+j), \sqrt{\frac{1}{26}}(3+j, 7+3j), \sqrt{\frac{1}{26}}(5+j, 5+3j), \sqrt{\frac{1}{26}}(5+j, 7+j) \end{array} \right\}$
64QAM	$\left\{ \begin{array}{l} \sqrt{\frac{1}{26}}(5+j, 7+3j), \sqrt{\frac{1}{26}}(5+3j, 7+3j), \sqrt{\frac{1}{26}}(5+3j, 7+3j), \sqrt{\frac{1}{26}}(7+j, 7+3j) \\ \sqrt{\frac{1}{42}}(1+j, 1+j), \sqrt{\frac{1}{42}}(1+j, 3+j), \sqrt{\frac{1}{42}}(1+j, 5+j), \sqrt{\frac{1}{42}}(1+j, 5+3j), \\ \sqrt{\frac{1}{42}}(1+j, 7+j), \sqrt{\frac{1}{42}}(1+j, 7+3j), \sqrt{\frac{1}{42}}(1+j, 7+5j), \sqrt{\frac{1}{42}}(3+j, 5+j), \\ \sqrt{\frac{1}{42}}(3+j, 5+3j), \sqrt{\frac{1}{42}}(3+j, 7+j), \sqrt{\frac{1}{42}}(3+j, 7+3j), \sqrt{\frac{1}{42}}(3+j, 7+5j), \\ \sqrt{\frac{1}{42}}(5+j, 5+3j), \sqrt{\frac{1}{42}}(5+j, 7+j), \sqrt{\frac{1}{42}}(5+j, 7+3j), \sqrt{\frac{1}{42}}(5+j, 7+5j), \\ \sqrt{\frac{1}{42}}(5+3j, 7+j), \sqrt{\frac{1}{42}}(5+3j, 7+3j), \sqrt{\frac{1}{42}}(5+3j, 7+5j), \sqrt{\frac{1}{42}}(7+j, 7+3j), \\ \sqrt{\frac{1}{42}}(7+j, 7+5j), \sqrt{\frac{1}{42}}(7+3j, 7+5j) \end{array} \right\}$

 TABLE III  
 CHANNEL PARAMETERS APPLIED IN EXAMPLES 2 AND 3.

MP#	$\beta$	$\theta_t$	$\theta_r$
1	0.9356	2	2.0
2	-0.2807	2.05	1.6
3	0.1871	1.2	2.4
4	-0.0936	3	2.45
5	0.0468	0.4	2.8

 TABLE IV  
 CANDIDATE SOLUTIONS OF  $\iota_2$  FOR EXAMPLE 3 AND THEIR ACHIEVABLE MINIMAL ED,  $\min\{J_{l_1, m_1, l_2, m_2}\}$ .

Candidates of $\iota_{\text{opt},2}$	Achievable $\min\{J_{l_1, m_1, l_2, m_2}\}$
$\frac{3\lambda_1}{(\sqrt{2}-1)^2\lambda_2}$	0.4497
$\frac{(1+2\sqrt{2})\lambda_1}{\lambda_2}$	0.8466
$\frac{\lambda_1}{\lambda_2}$	2.2520
$\frac{\lambda_2}{\lambda_1}$	2.9869
$\frac{(1+2\sqrt{2})\lambda_2}{(\sqrt{2}-1)^2\lambda_1}$	5.5460

Because  $\left| (1+3j) - \frac{1+j}{\sqrt{2}} \right|^2 > 1$ ,  $\frac{|1+j|^2}{2} = 1$ ,  
 $\left| (1+j) - \frac{1+3j}{\sqrt{2}} \right|^2 > 1$ ,  $\frac{|1+3j|^2}{2} > 1$ ,  $\left(1 - \frac{1}{\sqrt{2}}\right)^2 < 1$ ,  
 we obtain  $\mathcal{D}$  in (55).

Therefore, according to Theorem 2, the solution of (32) is one of the equations in (56). Then, the set of possible solutions are given by (57).

By investigating the five candidates, it is not difficult to figure out that  $\iota_{\text{opt},2} = \frac{(\sqrt{2}-1)^2\lambda_1}{3\lambda_2}$  maximizes  $\min\{J_{l_1, m_1, l_2, m_2}\}$ ,

as shown in TABLE. IV, and therefore it is the solution of the optimization problem (32).

By substituting  $\iota_{\text{opt},2} = \frac{(\sqrt{2}-1)^2\lambda_1}{3\lambda_2}$  into (32) and following some straightforward derivations, we obtain

$$\xi^2 = \left[ \frac{3\lambda_2}{(\sqrt{2}-1)^2\lambda_1 + 3\lambda_2}, \frac{(\sqrt{2}-1)^2\lambda_1}{(\sqrt{2}-1)^2\lambda_1 + 3\lambda_2} \right], \quad (58)$$

$$\mathcal{D} = \left\{ \frac{2}{5}[\lambda_1, 0], \frac{2}{5}[0, \lambda_2], \frac{1}{5} \left[ \left(1 - \frac{1}{\sqrt{2}}\right)^2 \lambda_1, \frac{1}{2}\lambda_2 \right], \frac{1}{5} \left[ \frac{1}{2}\lambda_1, \left(1 - \frac{1}{\sqrt{2}}\right)^2 \lambda_2 \right] \right\}. \quad (55)$$

$$\begin{cases} \frac{2}{5}\lambda_2\iota_2 = \frac{2}{5}\lambda_1, \\ \frac{2}{5}\lambda_2\iota_2 = \frac{1}{5} \left[ \left(1 - \frac{1}{\sqrt{2}}\right)^2 \lambda_1 + \frac{1}{2}\lambda_2\iota_2 \right], \\ \frac{2}{5}\lambda_2\iota_2 = \frac{1}{5} \left[ \frac{1}{2}\lambda_1 + \left(1 - \frac{1}{\sqrt{2}}\right)^2 \lambda_2\iota_2 \right], \\ \frac{2}{5}\lambda_1 = \frac{1}{5} \left[ \left(1 - \frac{1}{\sqrt{2}}\right)^2 \lambda_1 + \frac{1}{2}\lambda_2\iota_2 \right], \\ \frac{2}{5}\lambda_1 = \frac{1}{5} \left[ \frac{1}{2}\lambda_1 + \left(1 - \frac{1}{\sqrt{2}}\right)^2 \lambda_2\iota_2 \right], \\ \frac{1}{5} \left[ \left(1 - \frac{1}{\sqrt{2}}\right)^2 \lambda_1 + \frac{1}{2}\lambda_2\iota_2 \right] = \frac{1}{5} \left[ \frac{1}{2}\lambda_1 + \left(1 - \frac{1}{\sqrt{2}}\right)^2 \lambda_2\iota_2 \right]. \end{cases} \quad (56)$$

$$\iota_{\text{opt},2} \in \left\{ \frac{(\sqrt{2}-1)^2\lambda_1}{3\lambda_2}, \frac{1}{1+2\sqrt{2}}\frac{\lambda_1}{\lambda_2}, \frac{\lambda_1}{\lambda_2}, (1+2\sqrt{2})\frac{\lambda_1}{\lambda_2}, \frac{3}{(\sqrt{2}-1)^2}\frac{\lambda_1}{\lambda_2} \right\}. \quad (57)$$

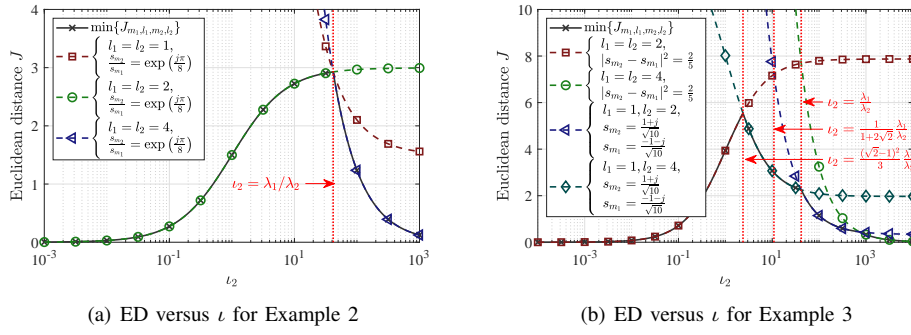


Fig. 2. Numerical validation of minimum ED maximization.

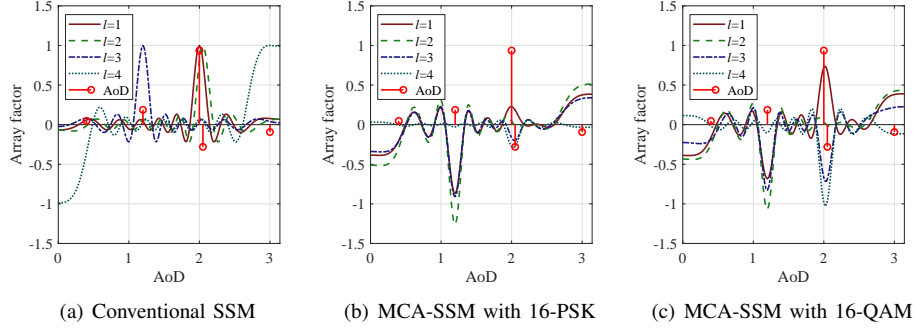


Fig. 3. Transmit array factors for the conventional SSM system and proposed MCA-SSM system.

and  $\mathbf{V}$  in (59). Thus, we obtain the MCA matrix  $\mathbf{W}$  as (60).

### B. Numerical results and discussions

To validate Theorem 1 and Theorem 2, the ED result versus  $l_2$  is illustrated in Fig. 2(a) and Fig. 2(b) for Example 2 and Example 3, respectively. In Fig. 2(a), it can be seen that  $l_{\text{opt},2} = \frac{\lambda_1}{\lambda_2}$  maximizes the minimal ED, i.e.,  $\min_{J_{l_1, m_1, l_2, m_2}}$  in (23), and in Fig. 2(b),  $l_{\text{opt},2} = \frac{(\sqrt{2}-1)^2 \lambda_1}{3 \lambda_2}$  maximizes the minimal ED.

Now, we take a deeper look into the transmit array factors for the conventional SSM system and the proposed MCA-

SSM, illustrated in Fig. 3. For the conventional SSM,  $\mathbf{W} = \mathbf{I}$ , and the beam is steered to only one MP component for each value of  $l$ . For the MCA-SSM with 16-PSK and 16-QAM,  $\mathbf{W}$  is given by (51) and (60), respectively, and MP components are aggregated for each value of  $l$ . This means that most of the four strongest MP components are steered for each value of  $l$ .

The task of the receiver is to detect the transmit array factor out of the illustrated four array factors while decoding  $\hat{l}$ . Unfortunately, the transmit array factors for  $l = 1$  and  $l = 2$  in the conventional SSM system are similar as the value of

$$\mathbf{V} = \begin{bmatrix} \frac{1}{\sqrt{2}} \sqrt{\frac{3\lambda_2}{(\sqrt{2}-1)^2 \lambda_1 + 3\lambda_2}} & \frac{1}{\sqrt{2}} \sqrt{\frac{(\sqrt{2}-1)^2 \lambda_1}{(\sqrt{2}-1)^2 \lambda_1 + 3\lambda_2}} & 0 & 0 \\ 0 & \sqrt{\frac{(\sqrt{2}-1)^2 \lambda_1}{(\sqrt{2}-1)^2 \lambda_1 + 3\lambda_2}} & 0 & 0 \\ -\frac{1}{\sqrt{2}} \sqrt{\frac{3\lambda_2}{(\sqrt{2}-1)^2 \lambda_1 + 3\lambda_2}} & \frac{1}{\sqrt{2}} \sqrt{\frac{(\sqrt{2}-1)^2 \lambda_1}{(\sqrt{2}-1)^2 \lambda_1 + 3\lambda_2}} & 0 & 0 \\ \sqrt{\frac{3\lambda_2}{(\sqrt{2}-1)^2 \lambda_1 + 3\lambda_2}} & 0 & 0 & 0 \end{bmatrix}. \quad (59)$$

$$\mathbf{W} = \begin{bmatrix} \frac{1}{\sqrt{2}} \sqrt{\frac{3\lambda_2}{(\sqrt{2}-1)^2 \lambda_1 + 3\lambda_2}} \mathbf{u}_1 + \frac{1}{\sqrt{2}} \sqrt{\frac{(\sqrt{2}-1)^2 \lambda_1}{(\sqrt{2}-1)^2 \lambda_1 + 3\lambda_2}} \mathbf{u}_2 \\ \sqrt{\frac{(\sqrt{2}-1)^2 \lambda_1}{(\sqrt{2}-1)^2 \lambda_1 + 3\lambda_2}} \mathbf{u}_2 \\ -\frac{1}{\sqrt{2}} \sqrt{\frac{3\lambda_2}{(\sqrt{2}-1)^2 \lambda_1 + 3\lambda_2}} \mathbf{u}_1 + \frac{1}{\sqrt{2}} \sqrt{\frac{(\sqrt{2}-1)^2 \lambda_1}{(\sqrt{2}-1)^2 \lambda_1 + 3\lambda_2}} \mathbf{u}_2 \\ \sqrt{\frac{3\lambda_2}{(\sqrt{2}-1)^2 \lambda_1 + 3\lambda_2}} \mathbf{u}_1 \end{bmatrix}. \quad (60)$$

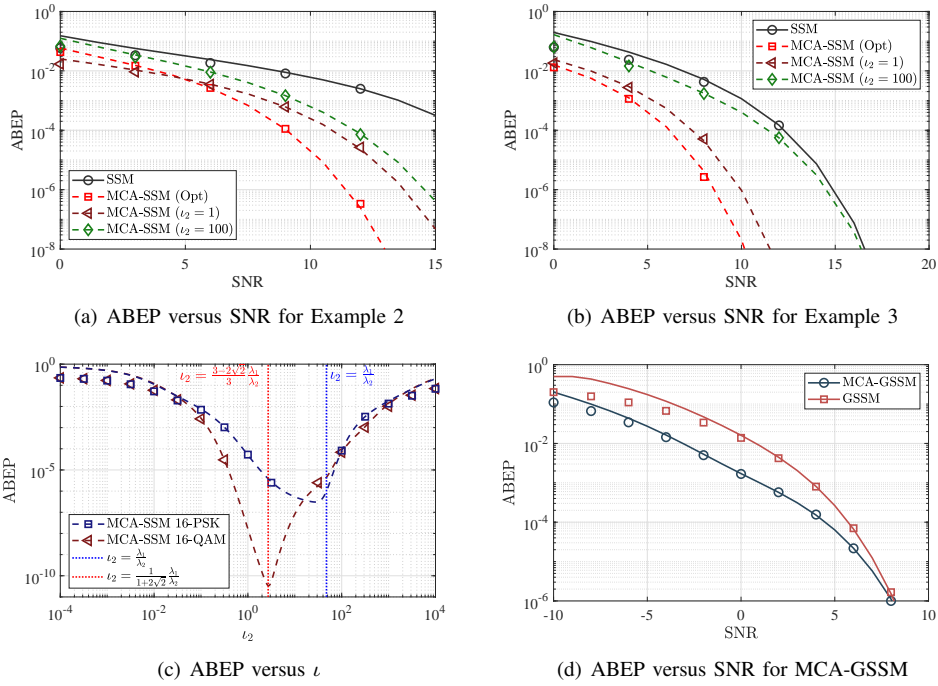


Fig. 4. Numerical validation of ABEP. Solid lines and dashed lines show the UUB computed by (20). Markers show simulation results.

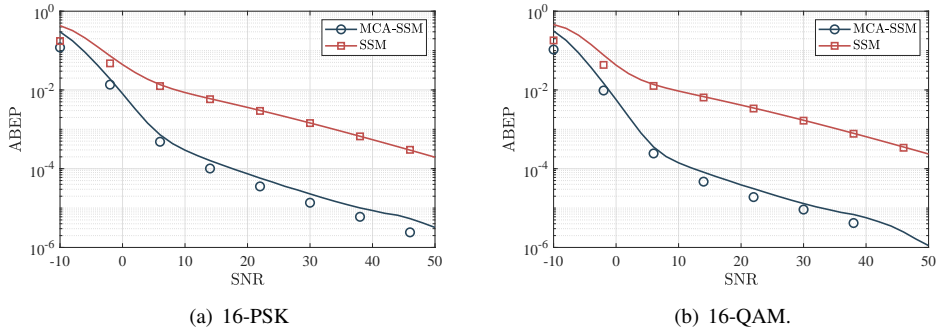


Fig. 5. Comparison between the proposed MCA-SSM with conventional SSM under stochastic channel model. Solid lines show the UUB computed by (20). Markers show simulation results.

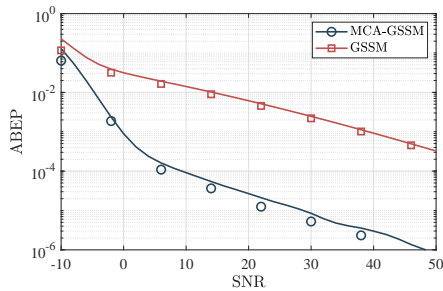


Fig. 6. Comparison between the proposed MCA-GSSM with conventional GSSM under stochastic channel model. Solid lines show the UUB computed by (20). Markers show simulation results.

$\theta_t(1)$  is close to the value of  $\theta_t(2)$ . Under this situation, ED for  $(l_1, l_2) = (1, 2)$  is small and leads to a large pairwise error performance  $P_{EP,H}(1, m_1, 2, m_1), \forall m_1 \in \{1, 2, \dots, M\}$ . In contrast, the shapes of four array factors for the proposed

MCA-SSM are quite different and easy to distinguish at the detector.

ABEPs of the proposed MCA-SSM system with  $l_{opt,2}$ ,  $l_2 = 1$  and  $l_2 = 100$  are illustrated in Fig. 4(a) and Fig. 4(b). It shows that  $l_{opt,2} = \frac{\lambda_1}{\lambda_2}$  and  $l_{opt,2} = \frac{(\sqrt{2}-1)^2}{3} \frac{\lambda_1}{\lambda_2}$ , obtained via Theorem 1 and Theorem 2, provide the lowest ABEP for Example 2 and Example 3, respectively. Overall, ABEPs for both Example 2 and Example 3 against  $l_2$  are illustrated in Fig. 4(c) to offer a clear validation of Theorem 1 and Theorem 2. It can be observed that the ABEP is minimized via the proposed approach.

Moreover, the performance enhancement by adopting the proposed MCA mechanism in the GSSM system is clearly shown in Fig. 4(d).

### C. Numerical validation in the stochastic channel model

In Fig. 4, we have investigated the performance of MCA-SSM with channel parameters listed in TABLE III. However,

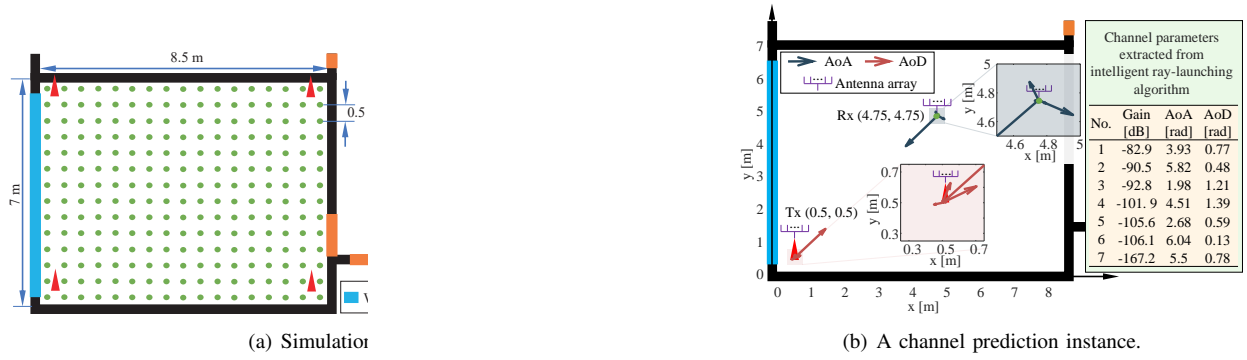


Fig. 7. IRLA-based channel prediction in a typical indoor environment.

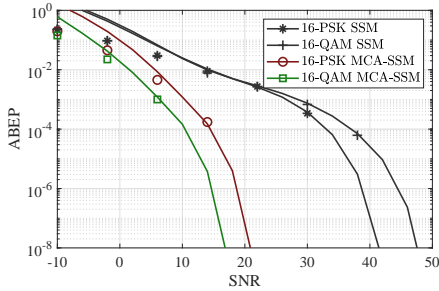


Fig. 8. Comparison between the proposed MCA-SSM with conventional SSM. Solid lines show the UUB computed by (20). Markers show simulation results.

channel parameters may vary with different locations of Tx and Rx in a typical building environment.

In this section, we apply the stochastic channel model in [9], [15]–[17] to investigate the performance of the proposed MSA-SSM system. More specifically, AoAs  $\theta_t$  and AoDs  $\theta_r$  of MPs are assumed to be i.i.d. uniformly distributed variables  $U(0, \pi)$ , respectively. The path gains  $\beta$  are assumed to be i.i.d. complex Gaussain distributed variables  $\mathcal{CN}(0, 1/N_{st})$ .

Under the stochastic channel model, the UUB on the ABEP of the proposed MCA-SSM system is analyzed in Fig. 5, where  $N_t = N_r = 16$ ,  $d_t = d_r = 0.5\eta$ ,  $N_s = 4$ ,  $L = 4$ ,  $N_{st} = 5$ , solid lines show the UUB computed by (20), and markers show simulation results. Meanwhile, the performance of the MCA-GSSM system with QPSK signal constellation is validated in Fig. 6.

Case studies and analysis using the stochastic channel model in this section provide proof-of-principle evaluation for the proposed MCA-SSM system. Beyond these case studies, there is a need to evaluate and compare the proposed MCA-SSM systems before deployment in a more practical environment.

## VI. NUMERICAL ANALYSIS IN A TYPICAL INDOOR ENVIRONMENT

Evaluation and comparison of the proposed MCA-SSM system considering environmental factors should be taken into account carefully before network deployment. Especially, evaluation in an indoor environment is crucial as most wireless traffics take place indoors [26]–[31]. In this section, we apply the deterministic channel model as a powerful tool to evaluate

the performance of the proposed MCA-SSM systems in a typical indoor environment [32].

### A. Channel prediction

The indoor environment under consideration is illustrated in Fig. 7(a). The IRLA, which has been validated via practical measurement [33], [34], is employed to predict indoor propagation channels.

In the prediction, the resolution is set as 0.5 m to achieve a good tradeoff between computational complexity and prediction accuracy. There are four Tx antenna arrays, located at four corners of the room, respectively. The IRLA slices the propagation environment into small cube units with a dimension of 0.5 m  $\times$  0.5 m  $\times$  0.5 m, and predicts channels between the Tx and centers of all cubes. The height of both Tx and Rx is set as 1 m above the floor. Channel prediction is carried out in the frequency band of 37–41.5 GHz. The Rx array visits all cube centers with a height of 1 m and computes the ergodic performance of SSM accordingly.

With 4 Tx positions and 238 Rx positions, there are  $N_l = 952$  links in total. The index of a link is denoted by  $n_l \in \{1, 2, \dots, 952\}$ . In each channel prediction, we obtain channel parameters including the number of MP components  $N_{ts}$ , the gain of each MP component  $\beta$ , AoD of each MP component  $\theta_r$ , and AoA of each MP component  $\theta_t$ . In the example shown in Fig. 7(b), Tx and Rx are located at (0.5, 0.5) and (4.75, 4.75), respectively. Seven MP components are present in this link. For all the other links, the IRLA is applied to extract channel parameters with the same data format.

### B. Numerical results

The UUB on the ABEP of the proposed MCA-SSM system is systematically analyzed and compared in the indoor environment illustrated in Fig. 7. Parameters of both the conventional SSM and the proposed MCA-SSM in this section are provided in TABLE V unless otherwise specified.

The ABEP of the proposed MCA-SSM is compared with that of the conventional SSM in Fig. 8. It is shown that the proposed MCA-SSM system outperforms the conventional SSM system significantly in terms of ABEP. To achieve an ABEP of  $10^{-6}$ , the proposed MCA-SSM with 16-PSK requires nearly 20 dB less transmit power than the conventional

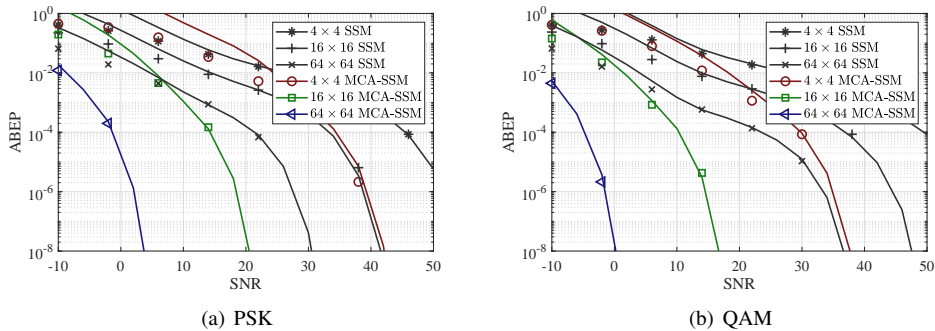


Fig. 9. Comparison of MCA-SSM with different scales of antenna arrays, with solid lines showing the UUB computed by (20), and markers showing simulation results.

TABLE V  
PARAMETERS IN NUMERICAL RESULTS.

Parameter	Description	Value
$N_r$	Number of Rx antennas	16
$N_t$	Number of Tx antennas	16
$d_t$	Spacing of Tx antenna elements	$0.5\eta$
$d_r$	Spacing of Rx antenna elements	$0.5\eta$
$N_s$	Candidate MP components	4
$L$	Candidate combinations of MP components	4

SSM, while the MCA-SSM with 16-QAM requires nearly 30 dB less. It reveals that conventional SSM systems suffer from both low cluster gain and inter-MP interference significantly. On the one hand, assumptions in [9, Eq. (2)] and [15, Eq. (4)] are not applicable for a MIMO system with relatively small-size antenna arrays. On the other hand, the assumption of  $\beta \sim \mathcal{CN}(0, \mathbf{I})$ , applied in [9], [12]–[15], overestimates the performance of conventional SSM systems. Fortunately, the proposed MCA-SSM systems overcome both problems effectively.

Then, the impact of antenna array size on the ABEP is shown in Fig. 9. It can be seen that the ABEP can be effectively reduced by increasing the scale of the antenna array for both systems. Nevertheless, more gain can be achieved via adding antenna elements for the proposed MCA-SSM system in comparison with the conventional SSM. In Fig. 9, the gain of the proposed MCA-SSM and the conventional SSM via scaling up the antenna array from  $4 \times 4$  to  $16 \times 16$  are, respectively, nearly 20 dB and 10 dB at  $\text{ABEP} = 10^{-6}$ . This result reveals that the bit error performance of conventional SSM suffers from MP components with low gains, even though they are well resolved via large-scale antenna arrays at both the Tx and the Rx.

Inspired by Fig. 4, it seems that the MCA mechanism without the optimisation of  $\iota$ , where the MCA matrix  $\mathbf{W}$  is easy to compute, could still achieve a relatively good bit error performance. To test this, Fig. 10 illustrates ABEPs of the MCA-SSM with optimal  $\iota_{2,\text{opt}}$ ,  $\iota_2 = \lambda_1/\lambda_2$ , and  $\iota_2 = 1$ , respectively. In Fig. 10, the 16-QAM signal constellation is applied. Surprisingly, the proposed MCA-SSM system with  $\iota_2 = \lambda_1/\lambda_2$  and  $\iota_2 = 1$  still significantly outperforms the conventional SSM system. It is shown that SNR losses due to suboptimal  $\iota_2 = \lambda_1/\lambda_2$  and  $\iota_2 = 1$  are, respectively, only 2.5

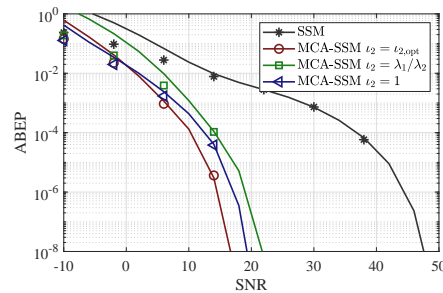


Fig. 10. Performance of MCA-SSM with optimal  $\iota_{2,\text{opt}}$ , suboptimal  $\iota_2 = \lambda_1/\lambda_2$ , and suboptimal  $\iota_2 = 1$ . Solid lines show the UUB computed by (20). Markers show simulation results.

dB and 4.5 dB at  $\text{ABEP} = 10^{-6}$ . Therefore, we can sacrifice the optimality of  $\iota_2$  to reduce implementation complexity in the designed MCA-SSM in case the computation resources are rather limited.

## VII. CONCLUSIONS

This paper proposes a new SSM system with a novel MCA mechanism introduced and the involved MCA matrix is analytically optimized to minimize the ABEP. The proposed approach is validated via both analytical UUB on the ABEP and Monte-Carlo simulations. The ABEP of the proposed MCA-SSM system is also systematically evaluated based on indoor channel predictions using IRLA. All the results show that the proposed MCA-SSM system outperforms the SSM system significantly, and can be considered as a promising candidate for 5G/B5G modulation systems with MIMO antenna arrays at both the transmitter and the receiver.

Possible future research topics along this line of research include applying this work to near-field massive MIMO scenarios [40] based on Green's function and electromagnetic information theory [41]–[43], considering how to effectively exploit polarization-domain resources to further enhance the performance of the MCA-SSM system, designing adaptive MCA-SSM system by adapting the modulation parameter to specific channel realization following [14], and analysis and reduction of computational complexity of the MCA algorithm by applying approaches in [7], [8].

APPENDIX A  
 PROOF OF THEOREM 1

The objective of solving (32) is to find the optimal  $\xi$  that maximizes  $J_{l_1, m_1, l_2, m_2}$ , which is denoted by

$$J_{\min} \triangleq \min_{\substack{(l_1, m_1) \neq (l_2, m_2) \\ 1 \leq l_1 \leq L, l_1 \in \mathbb{N}^+ \\ 1 \leq m_1 \leq M, m_1 \in \mathbb{N}^+ \\ 1 \leq l_2 \leq L, l_2 \in \mathbb{N}^+ \\ 1 \leq m_2 \leq M, m_2 \in \mathbb{N}^+}} J_{l_1, m_1, l_2, m_2}. \quad (61)$$

Consider

$$\xi^2 = \xi^2(1)\iota, \quad (62)$$

where

$$\iota = [1, \iota_2, \dots, \iota_{N_{s,a}}], \quad (63)$$

and

$$\iota_\kappa \triangleq \frac{\xi^2(\kappa)}{\xi^2(1)}. \quad (64)$$

Then, as long as

$$\xi^2(1) = \frac{1}{\sum_{\kappa=1}^{N_{s,a}} \iota_\kappa}, \quad (65)$$

we can directly calculate  $\xi^2$  with its associate  $\iota$  using (32). As a result, the ED for given  $\iota$  can be expressed as

$$J_{l_1, m_1, l_2, m_2} = \frac{\sum_{\kappa=1}^{N_{s,a}} \iota_\kappa \epsilon_{l_1, m_1, l_2, m_2}(\kappa)}{\sum_{\kappa=1}^{N_{s,a}} \iota_\kappa}, \quad (66)$$

where

$$\epsilon_{l_1, m_1, l_2, m_2} \triangleq \lambda \odot |\mathbf{v}_{l_1} s_{m_1} - \mathbf{v}_{l_2} s_{m_2}|^2. \quad (67)$$

Therefore, (32) can be reformulated as

$$\begin{aligned} \text{maximize} \quad & \min_{\substack{(l, m) \neq (\hat{l}, \hat{m}) \\ 1 \leq l \leq L, l \in \mathbb{N}^+ \\ 1 \leq m \leq M, m \in \mathbb{N}^+ \\ 1 \leq \hat{l} \leq L, \hat{l} \in \mathbb{N}^+ \\ 1 \leq \hat{m} \leq M, \hat{m} \in \mathbb{N}^+}} \frac{\sum_{\kappa=1}^{N_{s,a}} \iota_\kappa \epsilon_{l_1, m_1, l_2, m_2}(\kappa)}{\sum_{\kappa=1}^{N_{s,a}} \iota_\kappa}, \\ \text{s.t.} \quad & \iota_{2:N_{s,a}} \in (\mathbb{R}^+)^{N_{s,a}-1}. \end{aligned} \quad (68)$$

Note that the value of  $J_{l_1, m_1, l_2, m_2}$  is determined by both  $\epsilon_{l_1, m_1, l_2, m_2}$  and  $\iota$ . There are as many as  $(LM)^2 - 1$  sets of  $\epsilon_{l_1, m_1, l_2, m_2}$ . The following two challenging questions need to be addressed to solve (68).

- Challenge 1: Which  $\epsilon_{l_1, m_1, l_2, m_2}$  can possibly form a candidate solution of  $J_{\min}$  regardless of  $\iota$ ? For two values of  $\epsilon_{l_1, m_1, l_2, m_2}$ , denoted by  $\epsilon_{l_1, A, m_1, A, l_2, A, m_2, A}$  and  $\epsilon_{l_1, B, m_1, B, l_2, B, m_2, B}$ , if  $J_{l_1, A, m_1, A, l_2, A, m_2, A} > J_{l_1, B, m_1, B, l_2, B, m_2, B}, \forall \iota$ , then  $J_{l_1, A, m_1, A, l_2, A, m_2, A}$  is not a possible candidate solution.
- Challenge 2: How to find the optimal solution of  $\iota_{\text{opt}}$  that maximizes  $J_{\min}$ , provided candidate solutions of  $\epsilon_{l_1, m_1, l_2, m_2}$  calculated by addressing Challenge 1?

Challenge 1 is addressed as follows. Note that  $J_{l_1, m_1, l_2, m_2}$  has two types for  $l_1 = l_2$  and  $l_1 \neq l_2$ , respectively [35]. Then, we have

$$J_{\min} = \min\{J_{\min, \text{Mod}}, J_{\min, \text{MC}}\}, \quad (69)$$

where

$$J_{\min, \text{Mod}} \triangleq \min_{\substack{m_1 \neq m_2 \\ 1 \leq l_1 \leq L, l_1 \in \mathbb{N}^+ \\ 1 \leq m_1 \leq M, m_1 \in \mathbb{N}^+ \\ 1 \leq m_2 \leq M, m_2 \in \mathbb{N}^+}} J_{l_1, m_1, l_1, m_2}, \quad (70)$$

$$J_{\min, \text{MC}} \triangleq \min_{\substack{1 \leq l_1 \leq L, l_1 \in \mathbb{N}^+ \\ 1 \leq m_1 \leq M, m_1 \in \mathbb{N}^+ \\ 1 \leq l_2 \leq L, l_2 \in \mathbb{N}^+, l_2 \neq l_1 \\ 1 \leq m_2 \leq M, m_2 \in \mathbb{N}^+}} J_{l_1, m_1, l_2, m_2}. \quad (71)$$

Then the statement “ $\epsilon_{l_1, m_1, l_2, m_2}$  forms a candidate solution of either  $J_{\min, \text{Mod}}$  or  $J_{\min, \text{MC}}$ .” is a necessary condition for the statement “ $\epsilon_{l_1, m_1, l_2, m_2}$  forms a candidate solution of  $J_{\min}$ .”. Therefore, candidate solutions of  $J_{\min, \text{MC}}$  is the union of candidate solutions to both  $J_{\min, \text{Mod}}$  and  $J_{\min, \text{MC}}$ .

Candidate solutions of  $J_{\min, \text{Mod}}$  and  $J_{\min, \text{MC}}$  for the PSK signal constellation with given  $\iota$  are derived as follows.

According to (70), we have (72). For the PSK signal constellation, we have

$$\min_{\substack{m \neq \hat{m} \\ 1 \leq m \leq M, m \in \mathbb{N}^+ \\ 1 \leq \hat{m} \leq M, \hat{m} \in \mathbb{N}^+}} \{|s_{\hat{m}} - s_m|\} = 2 \sin\left(\frac{\pi}{M}\right) \quad (73)$$

By substituting (73) into (72), we obtain that

$$\epsilon_{l_1, m_1, l_1, m_2} \in \left\{4(\lambda \odot |\mathbf{v}_{l_1}|^2) \sin^2\left(\frac{\pi}{M}\right)\right\}. \quad (74)$$

forms candidate solutions of  $J_{\min, \text{Mod}}$ , and we have (75).

$$\begin{aligned} J_{\min, \text{Mod}} &= \min_{\substack{m_1 \neq m_2 \\ 1 \leq l_1 \leq L, l_1 \in \mathbb{N}^+ \\ 1 \leq m_1 \leq M, m_1 \in \mathbb{N}^+ \\ 1 \leq m_2 \leq M, m_2 \in \mathbb{N}^+}} \left\{ \sum_{\kappa=1}^{N_s} \xi^2(\kappa) \lambda_\kappa |\mathbf{v}_{l_1}(\kappa) s_{m_1} - \mathbf{v}_{l_1}(\kappa) s_{m_2}|^2 \right\} \\ &= \min_{\substack{m_1 \neq m_2 \\ 1 \leq m_1 \leq M, m_1 \in \mathbb{N}^+ \\ 1 \leq m_2 \leq M, m_2 \in \mathbb{N}^+}} \{|s_{m_1} - s_{m_2}|^2\} \min_{1 \leq l_1 \leq L, l_1 \in \mathbb{N}^+} \left\{ \sum_{\kappa=1}^{N_s} \xi^2(\kappa) \lambda_\kappa |\mathbf{v}_{l_1}(\kappa)|^2 \right\}. \end{aligned} \quad (75)$$

According to the definition of  $J_{\min,MC}$  in (71), we have (76).

Note that

$$\begin{aligned} & \sum_{\kappa=1}^{N_{s,a}} \xi^2(\kappa) \lambda_{\kappa} |\mathbf{v}_{l_1}(\kappa) s_{m_1} - \mathbf{v}_{l_2}(\kappa) s_{m_2}|^2 \\ &= |s_{m_1}|^2 \sum_{\kappa=1}^{N_{s,a}} \xi^2(\kappa) \lambda_{\kappa} \mathbf{v}_{l_1}^2(\kappa) \\ &+ |s_{m_2}|^2 \sum_{\kappa=1}^{N_{s,a}} \xi^2(\kappa) \lambda_{\kappa} \mathbf{v}_{l_2}^2(\kappa) \\ &- 2\mathcal{R}[s_{m_1} s_{m_2}^*] \sum_{\kappa=1}^{N_{s,a}} \xi^2(\kappa) \lambda_{\kappa} \mathbf{v}_{l_1}(\kappa) \mathbf{v}_{l_2}(\kappa). \end{aligned} \quad (77)$$

For PSK signal constellation,

$$\begin{cases} |s_{m_1}|^2 = |s_{m_2}|^2 = 1, \\ \mathcal{R}[s_{m_1} s_{m_2}^*] = \cos\left(\frac{2\pi(m_1 - m_2)}{M}\right). \end{cases} \quad (78)$$

Thus, we have

$$\begin{aligned} & \sum_{\kappa=1}^{N_{s,a}} \xi^2(\kappa) \lambda_{\kappa} |\mathbf{v}_{l_1}(\kappa) s_{m_1} - \mathbf{v}_{l_2}(\kappa) s_{m_2}|^2 \\ &= \sum_{\kappa=1}^{N_{s,a}} \xi^2(\kappa) \lambda_{\kappa} \mathbf{v}_{l_1}^2(\kappa) + \sum_{\kappa=1}^{N_{s,a}} \xi^2(\kappa) \lambda_{\kappa} \mathbf{v}_{l_2}^2(\kappa) \\ &- 2 \cos\left(\frac{2\pi(m_1 - m_2)}{M}\right) \sum_{\kappa=1}^{N_{s,a}} \xi^2(\kappa) \lambda_{\kappa} \mathbf{v}_{l_1}(\kappa) \mathbf{v}_{l_2}(\kappa). \end{aligned} \quad (79)$$

From (79), we see that  $\sum_{\kappa=1}^{N_{s,a}} \xi^2(\kappa) \lambda_{\kappa} |\mathbf{v}_{l_1}(\kappa) s_{m_1} - \mathbf{v}_{l_2}(\kappa) s_{m_2}|^2$  is minimized by  $\frac{2\pi(m_1 - m_2)}{M} = 0$  and

$\frac{2\pi(m_1 - m_2)}{M} = \pi$  while  $\sum_{\kappa=1}^{N_{s,a}} \xi^2(\kappa) \lambda_{\kappa} \mathbf{v}_{l_1}(\kappa) \mathbf{v}_{l_2}(\kappa) > 0$  and

$\sum_{\kappa=1}^{N_{s,a}} \xi^2(\kappa) \lambda_{\kappa} \mathbf{v}_{l_1}(\kappa) \mathbf{v}_{l_2}(\kappa) \leq 0$ , respectively.

Then, we conclude that for the PSK signal constellation, we have (80). By substituting (80) into (76), we obtain that

$$\epsilon_{l_1, m_1, l_2, m_2} \in \{\lambda \odot |\mathbf{v}_{l_1} \pm \mathbf{v}_{l_2}|^2\}, \quad (81)$$

forms candidate solutions of  $J_{\min,MC}$  as (82).

We can see the optimal solution of (68) must be formed by an  $\epsilon$  in either set (74) or set (81), and thus the candidate  $\epsilon$  is in the union of both sets, which is denoted by  $\mathcal{D}_0$  and summarized in (36) and (37).

Moreover, for a given  $\epsilon \in \mathcal{D}_0$ , if  $\epsilon(\kappa) \geq \epsilon'(\kappa), \forall \kappa, \exists \epsilon' \in \mathcal{D}_0, \epsilon' \neq \epsilon$ ,  $\epsilon$  always forms a greater  $J_{l_1, m_1, l_2, m_2}$  than  $\epsilon'$ , and can not be the solution of (69). Therefore, it needs to be excluded from the candidate set of  $\epsilon$ , and thus we have (35).

Challenge 2 is addressed via the following Lemma 1.

**Lemma 1. Monotonicity of  $J_{l_1, m_1, l_2, m_2}$ .**  $J_{l_1, m_1, l_2, m_2}$  is monotonous to  $\iota_{\kappa_0}, \forall 1 < \kappa_0 \leq N_{s,a}$ , for a given  $(l_1, m_1, l_2, m_2)$ .

*Proof:* See Appendix C. ■

Due to the monotonicity, the optimal solution of  $\iota$ , which contains  $N_{s,a} - 1$  unknown numbers, surely be one of intersections of  $N_{s,a} - 1$  sets of  $J_{l_1, m_1, l_2, m_2}$  out of all candidates in (75) and (76). Then, the intersection of  $J_{l_1, m_1, l_2, m_2} = \epsilon_{l_1, m_1, l_2, m_2} \iota^T$  can be computed by (34).

After addressing Challenge 1 and Challenge 2, Theorem 1 is proved.

## APPENDIX B PROOF OF THEOREM 2

It is worth noting that (62)-(72), (76)-(77), and Lemma 1 hold for the QAM signal constellation as well. However,

$$J_{\min,Mod} = \min_{1 \leq l_1 \leq L, l_1 \in \mathbb{N}^+} \left\{ 4 \sum_{\kappa=1}^{N_s} \xi^2(\kappa) \lambda_{\kappa} |\mathbf{v}_{l_1}(\kappa)|^2 \sin^2\left(\frac{\pi}{M}\right) \right\}. \quad (75)$$

$$J_{\min,MC} = \min_{\substack{1 \leq l_1 \leq L, l_1 \in \mathbb{N}^+ \\ 1 \leq l_2 \leq L, l_2 \in \mathbb{N}^+, l_2 \neq l_1}} \min_{\substack{1 \leq m_1 \leq M, m_1 \in \mathbb{N}^+ \\ 1 \leq m_2 \leq M, m_2 \in \mathbb{N}^+}} \left\{ \sum_{\kappa=1}^{N_s} \xi^2(\kappa) \lambda_{\kappa} |\mathbf{v}_{l_1}(\kappa) s_{m_1} - \mathbf{v}_{l_2}(\kappa) s_{m_2}|^2 \right\}. \quad (76)$$

$$\begin{aligned} & \min_{\substack{1 \leq m_1 \leq M, m_1 \in \mathbb{N}^+ \\ 1 \leq m_2 \leq M, m_2 \in \mathbb{N}^+}} \left\{ \sum_{\kappa=1}^{N_s} \xi^2(\kappa) \lambda_{\kappa} |\mathbf{v}_{l_1}(\kappa) s_{m_1} - \mathbf{v}_{l_2}(\kappa) s_{m_2}|^2 \right\} \\ &= \begin{cases} \sum_{\kappa=1}^{N_{s,a}} \xi^2(\kappa) \lambda_{\kappa} (\mathbf{v}_{l_1}(\kappa) - \mathbf{v}_{l_2}(\kappa))^2, & \text{if } \sum_{\kappa=1}^{N_{s,a}} \xi^2(\kappa) \lambda_{\kappa} \mathbf{v}_{l_1}(\kappa) \mathbf{v}_{l_2}(\kappa) > 0, \\ \sum_{\kappa=1}^{N_{s,a}} \xi^2(\kappa) \lambda_{\kappa} (\mathbf{v}_{l_1}(\kappa) + \mathbf{v}_{l_2}(\kappa))^2, & \text{if } \sum_{\kappa=1}^{N_{s,a}} \xi^2(\kappa) \lambda_{\kappa} \mathbf{v}_{l_1}(\kappa) \mathbf{v}_{l_2}(\kappa) \leq 0. \end{cases} \end{aligned} \quad (80)$$

$$J_{\min,MC} = \min_{\substack{1 \leq l_1 \leq L, l_1 \in \mathbb{N}^+ \\ 1 \leq l_2 \leq L, l_2 \in \mathbb{N}^+, l_2 \neq l_1}} \min_{\kappa=1}^{N_{s,a}} \left\{ \sum_{\kappa=1}^{N_{s,a}} \xi^2(\kappa) \lambda_{\kappa} (\mathbf{v}_{l_1}(\kappa) \pm \mathbf{v}_{l_2}(\kappa))^2 \right\}. \quad (82)$$

(73) and (78) do not hold for the QAM signal constellation. Therefore,  $J_{\min, \text{Mod}}$  in (72) and  $J_{\min, \text{MC}}$  in (76) need to be derived for QAM signal constellation to prove Theorem 2.

For QAM signal constellation, candidate solutions of  $J_{\min, \text{Mod}}$  and  $J_{\min, \text{MC}}$  are computed by the following Lemma 2 and Lemma 3, respectively.

**Lemma 2. Candidate solutions of  $J_{\min, \text{Mod}}$  for QAM signal constellation.**

For QAM signal constellation, candidate solutions of  $J_{\min, \text{Mod}}$  is formed by (83), and is given by (84).

*Proof:* For the QAM signal constellation, we have (85). By substituting (85) into (72), we obtain (84). ■

**Lemma 3. Candidate solutions of  $J_{\min, \text{MC}}$  for the QAM**

**signal constellation.**

$$\epsilon_{l_1, m_1, l_2, m_2} \in \{ |\mathbf{v}_{l_1} s_{m_1} \pm \mathbf{v}_{l_2} s_{m_2}|^2, (s_{m_1}, s_{m_2}) \in \mathcal{S}_m \} \quad (86)$$

forms candidate solutions of  $J_{\min, \text{MC}}$ , where the sets  $\mathcal{S}_m$  for square QAM and rectangular QAM signal constellations are calculated by (38) and (40), respectively. As such we obtain (87).

*Proof:* For QAM, we consider the following factor to reduce the search space of  $J_{\min, \text{MC}}$ .

- In a square  $M$ -QAM constellation diagram, there are  $\sqrt{M}/4 + M/8$  valid values of the amplitude of a constellation point. In a rectangular  $M$ -QAM constellation diagram, there are  $\sqrt{M}/32 + 3M/16$  valid values of the amplitude of a constellation point. They are indexed by  $\eta$ .

$$\epsilon_{l_1, m_1, l_1, m_2} \in \left\{ (\lambda \odot |\mathbf{v}_{l_1}|^2) \times \begin{cases} \frac{6}{M-1}, & \text{square QAM,} \\ \frac{24}{5M-4}, & \text{rectangular QAM.} \end{cases} \right\}. \quad (83)$$

$$J_{\min, \text{Mod}} = \min_{1 \leq l_1 \leq L, l_1 \in \mathbb{N}^+} \left\{ \sum_{\kappa=1}^{N_s} \xi^2(\kappa) \lambda_\kappa |\mathbf{v}_{l_1}(\kappa)|^2 \times \begin{cases} \frac{6}{M-1}, & \text{square QAM,} \\ \frac{24}{5M-4}, & \text{rectangular QAM.} \end{cases} \right\}. \quad (84)$$

$$\min_{\substack{m \neq \hat{m} \\ 1 \leq m \leq M, m \in \mathbb{N}^+ \\ 1 \leq \hat{m} \leq M, \hat{m} \in \mathbb{N}^+}} \{ |s_{\hat{m}} - s_m| \} = \begin{cases} \sqrt{\frac{6}{M-1}}, & \text{square QAM,} \\ \sqrt{\frac{24}{5M-4}}, & \text{rectangular QAM.} \end{cases} \quad (85)$$

$$J_{\min, \text{MC}} = \min_{\substack{1 \leq l_1 \leq L, l_1 \in \mathbb{N}^+ \\ 1 \leq l_2 \leq L, l_2 \in \mathbb{N}^+, l_2 \neq l_1}} \min_{(s_{m_1}, s_{m_2}) \in \mathcal{S}_m} \left\{ \sum_{\kappa=1}^{N_{s,a}} \xi^2(\kappa) \lambda_\kappa |\mathbf{v}_{l_1}(\kappa) s_{m_1} \pm \mathbf{v}_{l_2}(\kappa) s_{m_2}|^2 \right\}. \quad (87)$$

$$\mathcal{S}_m = \left\{ (s_1, s_2) \left| \begin{array}{l} 0 < \angle(s_1) \leq \pi/4, \angle(s_1) \leq \angle(s_2) \leq \angle(s_1) + \pi, \\ ((|s_1^*|, |s_2^*|) = (|s_1|, |s_2|) \wedge (\sin(\angle(s_2) - \angle(s_1)) < \sin(\angle(s_2^*) - \angle(s_1^*)))) \\ \vee ((|s_1^*| < |s_1|) \vee (|s_2^*| < |s_2|)) \wedge (\sin(\angle(s_2) - \angle(s_1)) = \sin(\angle(s_2^*) - \angle(s_1^*))) \end{array} \right. \right\}. \quad (88)$$

$$\min_{\substack{1 \leq m_1 \leq M, m_1 \in \mathbb{N}^+ \\ 1 \leq m_2 \leq M, m_2 \in \mathbb{N}^+}} \left\{ \sum_{\kappa=1}^{N_s} \xi^2(\kappa) \lambda_\kappa |\mathbf{v}_{l_1}(\kappa) s_{m_1} \pm \mathbf{v}_{l_2}(\kappa) s_{m_2}|^2 \right\} = \min_{(s_{m_1}, s_{m_2}) \in \mathcal{S}_m} \left\{ \sum_{\kappa=1}^{N_s} \xi^2(\kappa) \lambda_\kappa |\mathbf{v}_{l_1}(\kappa) s_{m_1} \pm \mathbf{v}_{l_2}(\kappa) s_{m_2}|^2 \right\}. \quad (89)$$

$$\frac{\partial J}{\partial l_{\kappa_0}} = \frac{\sum_{\kappa=1}^{N_{s,a}} l_\kappa \lambda_\kappa |\mathbf{v}_{l_1}(\kappa) s_{m_1} - \mathbf{v}_{l_2}(\kappa) s_{m_2}|^2}{\sum_{\kappa=1}^{N_{s,a}} l_\kappa} \quad (90)$$

$$= \xi^4(1) \sum_{\kappa \neq \kappa_0=1}^{N_{s,a}} l_\kappa \left( \begin{array}{l} \lambda_{\kappa_0} |\mathbf{v}_{l_1}(\kappa_0) s_{m_1} - \mathbf{v}_{l_2}(\kappa_0) s_{m_2}|^2 \\ -\lambda_\kappa |\mathbf{v}_{l_1}(\kappa) s_{m_1} - \mathbf{v}_{l_2}(\kappa) s_{m_2}|^2 \end{array} \right).$$

$$\frac{\partial J}{\partial l_{\kappa_0}} \left\{ \begin{array}{l} \geq 0, \quad \text{if } \sum_{\kappa \neq \kappa_0=1}^{N_{s,a}} l_\kappa \left( \begin{array}{l} \lambda_{\kappa_0} |\mathbf{v}_{l_1}(\kappa_0) s_{m_1} - \mathbf{v}_{l_2}(\kappa_0) s_{m_2}|^2 \\ -\lambda_\kappa |\mathbf{v}_{l_1}(\kappa) s_{m_1} - \mathbf{v}_{l_2}(\kappa) s_{m_2}|^2 \end{array} \right) \geq 0, \\ < 0, \quad \text{if } \sum_{\kappa \neq \kappa_0=1}^{N_{s,a}} l_\kappa \left( \begin{array}{l} \lambda_{\kappa_0} |\mathbf{v}_{l_1}(\kappa_0) s_{m_1} - \mathbf{v}_{l_2}(\kappa_0) s_{m_2}|^2 \\ -\lambda_\kappa |\mathbf{v}_{l_1}(\kappa) s_{m_1} - \mathbf{v}_{l_2}(\kappa) s_{m_2}|^2 \end{array} \right) < 0. \end{array} \right. \quad (91)$$

- For given values of amplitudes of two symbols, (77) is minimized by minimizing the angle between two straight lines. The first straight line is formed by  $s_{m_1}$  and the origin in the constellation diagram, and the second one is formed by  $s_{m_2}$  and the origin.
- For a given angle between two straight lines of the two symbols, (77) is minimized by minimizing the amplitudes of the two symbols.

Therefore, we can summarize possible pairs of  $s_1$  and  $s_2$  that minimize (77) as (88).

Following some straightforward derivations, we obtain (38) and (40) for the square QAM and the rectangular QAM signal constellations, respectively. Therefore, we obtain (89).

By substituting (89) into (76), we obtain (87). ■

### APPENDIX C PROOF OF LEMMA 1

To prove the monotonicity of  $J_{l_1, m_1, l_2, m_2; \kappa_0}$  to  $\kappa_0$ , we check  $\frac{\partial J}{\partial \kappa_0}$  computed by (90). As  $\sum_{\kappa \neq \kappa_0=1}^{N_{s,a}} \kappa \left( \begin{array}{l} \lambda_{\kappa_0} |\mathbf{v}_{l_1}(\kappa_0) s_{m_1} - \mathbf{v}_{l_2}(\kappa_0) s_{m_2}|^2 \\ - \lambda_{\kappa} |\mathbf{v}_{l_1}(\kappa) s_{m_1} - \mathbf{v}_{l_2}(\kappa) s_{m_2}|^2 \end{array} \right)$  is irrelevant to  $\kappa_0$ , we have (91). Therefore,  $J_{l_1, m_1, l_2, m_2; \kappa_0}$  is monotonous to  $\kappa_0$ ,  $\forall 1 < \kappa_0 \leq N_{s,a}$ , for a given  $(l_1, m_1, l_2, m_2)$ .

### REFERENCES

- [1] R. Y. Mesleh et al., "Spatial modulation," *IEEE Trans. Veh. Technol.*, vol. 57, no. 4, pp. 2228-2241, July 2008.
- [2] M. Di Renzo, et al., "Spatial modulation for multiple antenna wireless systems: A survey," *IEEE Commun. Mag.*, vol. 49, no. 12, pp. 182-191, Dec. 2011.
- [3] M. Di Renzo, et al., "Spatial modulation for generalized MIMO: Challenges, opportunities, and implementation," *Proc. IEEE*, vol. 102, no. 1, pp. 56-103, Jan. 2014.
- [4] P. Yang, et al., "Design guidelines for spatial modulation," *IEEE Commun. Surveys Tuts.*, vol. 17, no. 1, pp. 6-26, 1st Quart., 2015.
- [5] P. Yang et al., "Single-carrier SM-MIMO: A promising design for broadband large-scale antenna systems," *IEEE Commun. Surveys Tuts.*, vol. 18, no. 3, pp. 1687-1716, 3rd Quart., 2016.
- [6] S. Guo et al., "Asymptotic capacity for MIMO communications with insufficient radio frequency chains," *IEEE Trans. Commun.*, vol. 68, no. 7, pp. 4190-4201, July 2020.
- [7] J. Zhang et al., "Generalized polarization-space modulation," *IEEE Trans. Commun.*, vol. 68, no. 1, pp. 258-273, Jan. 2020.
- [8] J. Zhang et al., "Polarization shift keying (PolarSK): System scheme and performance analysis," *IEEE Trans. Veh. Technol.*, vol. 66, no. 11, pp. 10139-10155, Nov. 2017.
- [9] Y. Ding et al., "Spatial scattering modulation for uplink millimeter-wave system," *IEEE Commun. Lett.*, vol. 21, no. 10, pp. 2178-2181, Jul. 2017.
- [10] Y. Ding et al., "Millimeter wave adaptive transmission using spatial scattering modulation," *IEEE Int. Conf. Commun.*, pp. 1-6, May 2017.
- [11] Y. Ding et al., "Beam index modulation wireless communication with analog beamforming," *IEEE Trans. Veh. Technol.*, vol. 67, no. 7, pp. 6340-6354, July 2018.
- [12] S. Ruan et al., "Diversity analysis for spatial scattering modulation in millimeter wave MIMO system," *IEEE Int. Conf. Wireless Commun. Signal. Process.*, pp. 1-5, Sep. 2019.
- [13] Q. Li et al., "Polarized spatial scattering modulation," *IEEE Commun. Lett.*, vol. 23, no. 12, pp. 2252-2256, Dec. 2019.
- [14] J. Zhang "Adaptive spatial scattering modulation," *IEEE Trans. Wireless Commun.*, vol. 20, no. 10, pp. 6680-6690, Oct. 2021.
- [15] Y. Tu et al., "Generalized spatial scattering modulation for uplink millimeter wave MIMO system," *IEEE/CIC Int. Conf. Commun. in China*, pp. 22-27, Aug. 2018.
- [16] S. Guo et al., "Generalized beamspace modulation using multiplexing: A breakthrough in mmWave MIMO," *IEEE J. Sel. Areas Commun.*, vol. 37, no. 9, pp. 2014-2028, Sept. 2019.
- [17] Y. Jiang et al., "Generalized 3-D spatial scattering modulation," *IEEE Trans. Wireless Commun.*, vol. 21, no. 3, pp. 1570-1585, March 2022.
- [18] J. Zhang et al., "Bit error probability of spatial modulation over measured indoor channels," *IEEE Trans. Wireless Commun.*, vol. 13, no. 3, pp. 1380-1387, March 2014.
- [19] S. Guo et al., "Signal shaping for generalized spatial modulation and generalized quadrature spatial modulation," *IEEE Trans. Wireless Commun.*, vol. 18, no. 8, pp. 4047-4059, 2019.
- [20] S. Guo et al., "Signal shaping for non-uniform beamspace modulated mmWave hybrid MIMO communications," *IEEE Trans. Wireless Commun.*, vol. 19, no. 10, pp. 6660-6674, Oct. 2020.
- [21] Z. Zhao et al., "Performance analysis of the hybrid satellite-terrestrial relay network with opportunistic scheduling over generalized fading channels," *IEEE Trans. Veh. Technol.*, vol. 71, no. 3, pp. 2914-2924, March 2022.
- [22] O. Ayach et al., "Spatially sparse precoding in millimeter wave MIMO systems," *IEEE Trans. Wireless Commun.*, vol. 13, no. 3, pp. 1499-1513, Mar. 2014.
- [23] J. Jeganathan et al., "Spatial modulation: Optimal detection and performance analysis," *IEEE Commun. Lett.*, vol. 12, no. 8, pp. 545-547, Aug. 2008.
- [24] M. K. Simon and M. Alouini, *Digital communication over fading channels*, Hoboken, NJ, USA: Wiley, 2005.
- [25] A. Goldsmith, *Wireless communications*, Cambridge, UK: Cambridge University Press, 2005.
- [26] J. Zhang et al., "Fundamental wireless performance of a building," *IEEE Wireless Commun.*, vol. 29, no. 1, pp. 186-193, Feb. 2022.
- [27] J. Zhang et al., "Wireless performance evaluation of building layouts: Closed-form computation of figures of merit," *IEEE Trans. Commun.*, vol. 69, no. 7, pp. 4890-4906, July 2021.
- [28] J. Zhang et al., "Wireless energy efficiency evaluation for buildings under design based on analysis of interference gain," *IEEE Trans. Veh. Technol.*, vol. 69, no. 6, pp. 6310-24, June 2020.
- [29] Y. Zhang et al., "How friendly are building materials as reflectors to indoor LOS MIMO communications?" *IEEE Internet Things J.*, vol. 7, no. 9, pp. 9116-9127, Sep. 2020.
- [30] Y. Zhang et al., "Lower-bound capacity-based wireless friendliness evaluation for walls as reflectors," *IEEE Trans. Broadcast.*, vol. 67, no. 4, pp. 917-924, Dec. 2021.
- [31] Y. Zhang et al., "Effects of wall reflection on the per-antenna power distribution of ZF-precoded ULA for indoor mmWave MU-MIMO transmissions," *IEEE Commun. Lett.*, vol. 25, no. 1, pp. 13-17, Jan. 2021.
- [32] Z. Lai et al., "Intelligent ray launching algorithm for indoor scenarios," *Radioengineering*, vol. 20, no. 2, pp. 398-408, June 2011.
- [33] W. Yang et al., "Verification of an intelligent ray launching algorithm in indoor environments in the Ka-band," *Radio Science*, vol. 56, no. 9, pp. 1-11, Sept. 2021.
- [34] W. Yang et al., "Indoor measurement based verification of ray launching algorithm at the Ka-band," *XXXIIIrd General Assembly and Scientific Symposium of the International Union of Radio Science*, 2020, pp. 1-4.
- [35] M. Di Renzo and H. Haas, "Bit error probability of SM-MIMO over generalized fading channels," *IEEE Trans. Veh. Technol.*, vol. 61, no. 3, pp. 1124-1144, March 2012.
- [36] P. Yang et al., "Star-QAM signaling constellations for spatial modulation," *IEEE Trans. Veh. Technol.*, vol. 63, no. 8, pp. 3741-3749, Oct. 2014.
- [37] S. Fang et al., "Zero forcing assisted single layer beamforming for spatial modulation MIMO systems," *IEEE Trans. Veh. Technol.*, vol. 71, no. 4, pp. 4116-4128, April 2022.
- [38] A. Younis, et al., "Generalised spatial modulation," *44th Asilomar Conf. Signals Syst. Comput.*, pp. 1498-1502, 2010.
- [39] J. Fu, et al., "Generalised spatial modulation with multiple active transmit antennas," *IEEE Globecom Workshops*, pp. 839-844, 2010.
- [40] S. Guo et al., "Beamspace modulation for near field capacity improvement in XL-MIMO communications," *IEEE Wireless Commun. Lett.*, early access.
- [41] Z. Wan et al., "Mutual information for electromagnetic information theory based on random fields," *IEEE Trans. Commun.*, vol. 71, no. 4, pp. 1982-1996, 2023.
- [42] J. Zhu et al., "Electromagnetic information theory: Fundamentals, modeling, applications and open problems," arXiv preprint arXiv:2212.02882, 2022.
- [43] M. D. Migliore, "Horse (electromagnetics) is more important than horseman (information) for wireless transmission," *IEEE Trans. Ant. Prop.*, vol. 67, no. 4, pp. 2046-2055, 2019.



**Jiliang Zhang** is currently a full Professor at College of Information Science and Engineering, Northeastern University, Shenyang, China. He received the B.E., M.E., and Ph.D. degrees from the Harbin Institute of Technology, Harbin, China, in 2007, 2009, and 2014, respectively. He was an Associate Professor with the School of Information Science and Engineering, Lanzhou University from 2017 to 2019, and a researcher at the Department of Electrical Engineering, Chalmers University of Technology, Gothenburg, Sweden from 2017 to 2018, a Marie

Curie Research Fellow and a KTP associate at the Department of Electronic and Electrical Engineering, The University of Sheffield, Sheffield, UK from 2018 to 2022. His research interests include, but are not limited to wireless channel modeling, modulation system, relay system, vehicular communications, ultra-dense small cell networks, and smart environment modeling. He has pioneered systematic building wireless performance evaluation, modeling, and optimization, with the key concepts summarized in *Fundamental Wireless Performance of a Building*, IEEE Wireless Communications, 29(1), 2022. He is also the Academic Editor for *Wireless Communications and Mobile Computing* since 2019. He was the recipient of the IEEE Wireless Communications Letters Exemplary Reviewer Award in both 2021 and 2022.



**Wei Liu** received his BSc and LLB. degrees from Peking University, China, in 1996 and 1997, respectively, MPhil from the University of Hong Kong in 2001, and PhD from University of Southampton, UK, in 2003. He then worked as a postdoc first at Southampton and later at Imperial College London. In September 2005, he joined the Department of Electronic and Electrical Engineering, University of Sheffield, UK, first as a Lecturer and then a Senior Lecturer. Since September 2023, he has been a Reader at the School of Electronic Engineering and

Computer Science, Queen Mary University of London, UK. He has published 400+ journal and conference papers, five book chapters, and two research monographs titled “Wideband Beamforming: Concepts and Techniques” (Wiley, March 2010) and “Low-Cost Smart Antennas” (Wiley, March 2019), respectively. His research interests cover a wide range of topics in signal processing, with a focus on sensor array signal processing and its various applications, such as robotics and autonomous systems, human computer interface, radar, sonar, and wireless communications.

He is a member of the Digital Signal Processing Technical Committee of the IEEE Circuits and Systems Society (Chair for 2022-2024), the Sensor Array and Multichannel Signal Processing Technical Committee of the IEEE Signal Processing Society (SPS) (Chair for 2021-2022), the IEEE SPS Technical Directions Board (2021-2022), and the IEEE SPS Conference Board (2022-2023). He also acted as an associate editor for IEEE Trans. on Signal Processing, IEEE Access, and Journal of the Franklin Institute, and currently he is an Executive Associate Editor-in-Chief of the Frontiers of Information Technology and Electronic Engineering. He is an IEEE Distinguished Lecturer for the Aerospace and Electronic Systems Society (2023-2024).



**Alan Tennant** received the B.Eng. degree in electronic engineering and the Ph.D. degree in microwave engineering from The University of Sheffield, Sheffield, U.K., in 1985 and 1992, respectively. He was with BAE Systems, Stevenage, U.K. He then joined DERA, Farnborough, U.K., where he worked on phased-array antenna systems before taking up an academic post with Hull University, Hull, U.K. He returned to The University of Sheffield in 2001 as a Senior Lecturer with the Communications and Radar Group, where he is currently a Professor

and involved in research into techniques, materials, and signal processing for adaptive radar signature management, novel 3-D phased-array antenna topologies, acoustic array systems, and new research into time-modulated array antennas. He has published over 100 academic articles, including several invited articles on adaptive stealth technology. His research has attracted substantial funding from both industry and government sources.



**Weijie Qi** is currently a Research Data Scientist in Ranplan Wireless, Cambridge, U.K. Weijie Qi received the Ph.D. degree from the University of Sheffield, and finished his post-doctoral research from the University of Warwick. He is currently researching natural language processing, social media analytics and wireless network optimisation in urban and indoor areas.



**Jiming Chen** received his M.S. and Ph.D degree in communication and information system from University of Electronic and Science Technology, China in 2003 and 2006, respectively. Now he is a Principal Wireless Engineer and Manager of Wireless Research Group at Ranplan Wireless Network Design Ltd. (UK) from 2018. Prior to the time, he was a Head of Wireless Network Team and Senior Research Fellow at Ranplan from 2011, and a Research Scientist in Bell labs at Alcatel-Lucent Shanghai Bell Ltd. from 2006 to 2011, and then

became a Member of Alcatel-Lucent Technical Academy in 2010, where his research interests were the key techniques of cooperative processing and small cells for 3GPP LTE-A system. Currently, he focuses the research on 5G NR and WiFi 7 key technologies, such as 5G+AI, mmWave, Massive MIMO, and beamforming, for indoor and outdoor scenarios, and implementation in Ranplan planning and optimization tools. Up to now, he held about 30+ international patents and 30+ publications.



**Jie Zhang** has held the Chair in Wireless Systems at the Department of Electronic and Electrical Engineering, University of Sheffield, Sheffield, U.K., on a part-time basis, since January 2011. He is also the Founder, a Board Director and the Chief Scientific Officer of Ranplan Wireless, Cambridge, U.K., a public company listed on Nasdaq First North. Ranplan Wireless produces a suite of world leading indoor and the first joint indoor-outdoor radio access network planning tool – Ranplan Professional, which is being used by all the top 5 telecom equipment

vendors and the world’s largest mobile operators, system integrators and research organisations. Along with his students and colleagues, he has pioneered research in small cell and heterogeneous network and published some of the landmark papers and book on these topics, widely used by both academia and industry. Since 2010, he and his team have also developed ground-breaking work in smart radio environment and building wireless performance modelling, evaluation and optimisation, the key concepts of which were introduced in a paper titled “Fundamental Wireless Performance of a Building”, IEEE Wireless Communications, 29(1), 2022. His Google scholar citations are in excess of 8500 with an H-index of 40. He received a Ph.D. degree in industrial automation from East China University of Science and Technology, Shanghai, China, in 1995. Prior to joining the University of Sheffield, he had studied/worked with Imperial College London, Oxford University, and University of Bedfordshire, reaching a status of Senior Lecturer, Reader and Professor in 2002, 2005 and 2006, respectively.